MECHANICAL AND WEAR BEHAVIOR FOR ALUMINUM ALLOY REINFORCED WITH DUAL NANOPARTICULATE (TiO_2 + SiO_2)

MUSTAFA KHUDHAIR MOHSIN AL-GBURI

2022
MASTER THESIS
METALLURGICAL AND MATERIALS ENGINEERING

Thesis Advisors:
Prof. Dr. Hayrettin AHLATCI
Assist. Prof. Dr. Ali Mundher Mustafa ALDULAIMI

MECHANICAL AND WEAR BEHAVIOR FOR ALUMINUM ALLOY REINFORCED WITH DUAL NANOPARTICULATE (TiO_2 + SiO_2)

Mustafa Khudhair Mohsin Al-GBURI

T.C.
Karabuk University
Institute of Graduate Programs
Department of Metallurgical and Materials Engineering
Prepared as
Master Thesis

Thesis Advisors
Prof. Dr. Hayrettin AHLATCI
Assist. Prof. Dr. Ali Mundher Mustafa ALDULAIMI

KARABUK
July 2022

I certify that, in my opinion, the thesis submitted by Mustafa Khudhair Mohsin Al-Gburi titled“MECHANICAL AND WEAR BEHAVIOR FOR ALUMINUM ALLOY REINFORCED WITH DUAL NANOPARTICULATE (TiO2 + SiO2)” is fully adequate in scope and quality as a thesis for the degree of Master of Science.

Prof. Dr. Hayrettin AHLATCI .....
Thesis Advisor, Department of Metallurgical And Materials Engineering

This thesis is accepted by the examining committee with a unanimous vote in the Department of Metallurgical and Materials Engineering as a Master of Science thesis. July 17,2022

Examining Committee Members (Institutions)	Signature
Chairman : Prof. Dr. Hayrettin AHLATCI (KBU)	.....
Member : Assoc. Prof. Dr. Yunus TÜREN (KBU)	.....
Member : Prof. Dr. Mustafa ACARER (SELU)	(Online)
Member : Assist. Prof. Dr. Ali Mundher Mustafa (TECHUB)	(Online)
Member : Prof. Dr. Ismail ESEN (KBU)	.....

The degree of Master of Science by the thesis submitted is approved by the Administrative Board of the Institute of Graduate Programs, Karabuk University.

Prof. Dr. Hasan SOLMAZ .....
Director of the Institute of Graduate Programs

"I declare that all the information within this thesis has been gathered and presented under academic regulations and ethical principles, and I have, according to the requirements of these regulations and principles, cited all those which do not originate in this work as well."

Mustafa Khudhair Mohsin Al-GBUR

ABSTRACT

M. Sc. Thesis

MECHANICAL AND WEAR BEHAVIOR FOR ALUMINUM ALLOY REINFORCED WITH DUAL NANOPARTICULATE (TiO_2 + SiO_2).

Mustafa Khudhair Mohsin Al-GBURI

Karabük University
Institute of Graduate Programs
The Department of Metallurgical and Materials Engineering

Thesis Advisor
Prof. Dr. Hayrettin AHLATCI
Assist. Prof. Dr. Ali Mundher Mustafa ALDULAIMI

August 2022, 93 pages

This thesis is devoted to studying the influence of adding different weight ratios of TiO_2 and SiO_2 nanoparticles powder on the Al6061 alloy's mechanical characteristics and wear resistance. Composite materials containing different ratios of TiO_2 : SiO_2 (0.1:0, 0:0.1,0.1:0.1, 0.3:0, 0:0.3, 0.3:0.3, 0.5:0, 0:0.5, 0.5:0.5, 0.1:0.3, 0.1:0.5, 0.3:0.1, 0.3:0.5, 0.5:0.1, 0.5:0.3) were cast by the stirring method. The microstructure and phases are achieved through optical microscopy, SEM, and X-ray diffraction. The results displayed homogeneity in the base alloy's microstructure, where the reinforcing particles are distributed. The tensile and hardness Test conducted the mechanical properties. The ultimate tensile strength and yield strength increased by adding both TiO_2 and SiO_2 nanoparticles of more than0.5 wt%,the tensile strength

became 151.12MPa and the yield strength 76.87MPa. But the elongation decreased, and elongation became 9.61% compared to 31.39% in the base alloy. The hardness test results displayed that the hybrid composite having 0.5 wt% for both TiO_2 and SiO_2 nanoparticles had higher hardness than other composites and base alloys; the amount of hardness in 0.5%wt hybrid composite became 77.35HV compared to 68.88HV in the base alloy. The wear rate measurement by the pin on the disc device for both the basic alloy and the hybrid composite. The wear results showed a decrease in the wear rate at 0.5 wt% of both TiO_2 and SiO_2 nanoparticles containing composites as compared to the other composites and the base alloy samples,And it was worth0.82*10^-8 gm/cm compared to 1.82*10^-8gm/cm in the base alloy.

Key Words: Nanoparticles, Wear, Tensile, Hardness, TiO_2, SiO_2.

Science Code : 91512

ÖZET

ÇİFT NANOPARTİKÜL (TiO_2 + SiO_2) İLE GÜÇLENDİRİLMİŞ ALÜMİNYUM ALAŞIMI İÇİN MEKANİK VE AŞINMA DAVRANIŞI.

Mustafa Khudhair Mohsin Al-GBURI

Karabük Üniversitesi

Lisansüstü Eğitim Enstitüsü
Metalurji ve Malzeme Mühendisliği Anabilim Dalı

Tez Danışmanları
Prof. Dr. Hayrettin AHLATCI
Assist. Prof. Dr. Ali Mundher Mustafa ALDULAIMI

Ağustos 2022, 93 Sayfa

Bu makale, farklı ağırlık oranlarında TiO_2 ve SiO_2 nanoparçacık tozu eklenmesinin Al6061 alaşımının mekanik özellikleri ve korozyon direnci üzerindeki etkisini incelemeye ayrılmıştır. Farklı TiO_2 oranları içeren kompozit malzemeler: SiO_2 (0.1:0, 0.1:0.1, 0:0.1, 0.3:0, 0:0.3, 0.3:0.3, 0.5:0, 0:0.5, 0.5:0.5, 0.1:0.3, 0.1:0.5, 0.3:0.1, 0.3:0.5, 0.5:0.1, 0.5:0.3) karıştırma yöntemiyle dökülmüştür. Mikro yapı ve fazlar, optik mikroskopi, SEM ve X-ışını kırınımı yoluyla elde edilir. Sonuçlar, temel alaşımın mikro yapısındaki takviye edici parçacıkların dağılımında büyük ölçüde homojenlik elde edildiğini gösterdi. Çekme ve sertlik testi mekanik özellikleri gerçekleştirdi. Nihai çekme mukavemeti ve akma mukavemeti, ağırlıkça %0.5'e kadar hem TiO_2 hem de SiO_2 nanoparçacıklarının eklenmesiyle arttı, gerilme mukavemeti 151.12MPa ve akma mukavemeti 76.87MPa oldu. Ancak uzama azaldı ve uzama, baz alaşımdaki %31.39'a kıyasla %9.61 oldu. Sertlik testi sonuçları, ağırlıkça %0.5 hem TiO_2 hem de SiO_2 nanoparçacıkları içeren hibrit kompozitin

diğer kompozitlere ve baz alaşımlara göre daha yüksek sertliğe sahip olduğunu göstermiştir; ağırlıkça %0.5 hibrit kompozitteki sertlik miktarı, baz alaşımdaki 68.88HV'ye kıyasla 77.35HV oldu. Hem temel alaşım hem de hibrit kompozit için disk cihazı üzerindeki pim ile aşınma oranı ölçümü. Aşınma sonuçları, kompozit içeren hem TiO_2 hem de SiO_2 nanoparçacıklarının ağırlıkça %0.5'inde, diğer kompozitlere ve baz alaşım numunelerine kıyasla aşınma oranında bir azalma olduğunu gösterdi ve bu değer, diğer kompozitlere ve baz alaşım numunelerine göre 0,82*10^-8 gm/cm değerindeydi. Baz alaşımda 1.82*10^-8gm/cm.

Anahtar Kelimeler: Nanopartiküller, Aşınma, Çekme, Sertlik, TiO_2, SiO_2.

Bilim Kodu: 91512

ACKNOWLEDGMENT

In the beginning, I want to thank God for all the blessings He has given me. Then want to thank those who gave their lives for me, my father and mother, and the candle that lights my way in the darkness of life, my wife and children. I want to thank my advisor, Prof. Dr Hayrettin AHLATCI, and all thanks and appreciation to my teacher, brother, and friend, Dr Ali Mundher Mustafa, for his outstanding efforts, interest, and assistance in preparing this master's thesis. I thank my sisters, relatives, friends, and colleagues at university and work. I hope that I have made a small contribution to the development of this scientific sector.I dedicate this work to the souls of my four uncles and aunts, who I lost during the horrific COVID-19.

CONTENTS

Page

Page

Page

LIST OF FIGURES

Page

Page

Page

LIST OF TABLES

Page

SYMBOLS AND ABBREVITIONS INDEX

SYMBOLS

YS : Yielding Strength

UTS : Ultimate Tensile Strength

γ_{SV} : Solid-Vapor Surface Energies

γ_{SL} : Solid-Liquid Surface Energies

γ_{LV} : Liquid-Vapour Surface Energies

HV : Hardness Of Vickers

P : Load

D_{av} : Length Of Diagonal

SD : Slidingdistance

r : The distance between the specimen's and the disc's respective centers

n : Disc Rotational Speeds

t : Time

V : Velocity

ΔW : Weight of the specimen before and after the test, and its difference (g)

SD : Sliding Distance (cm)

ABBREVIATIONS

MMCs : Metal Matrix Composites

AMC : Aluminum Matrix Composites

MMNCs : Metal Matrix Nanocomposites

PM :Powder Metallurgy

SEM : Scanning Electron Microscopy

EDS : Energy Dispersive Spectrometry

XRD : X-Ray Diffraction

PART ONE

INTRODUCTION

The second most abundant metallic element on this planet is aluminum. It became a competitive engineering subject in the late 19th century.The difficulty of obtaining aluminum from its ore was the reason it was not employed sooner.

Aluminum and its alloys have several uses, ranging from very ductile soft packing sheets to the most difficult technical applications.One of the most versatile materials is aluminum and its alloys.Currently, available metallic materials are affordable and visually pleasing. In terms of structural metals, aluminum alloys are only second to steel in terms of use [1, 2].

The density of aluminum is just 2.7 g/cm^3, about one-third that of steel (7.83 g/cm^3). Combining this low weight with specific aluminum alloys' great strength (more excellent than that of structural steel)makes it possible to create sturdy, lightweight structures that are especially helpful for moving objects like spacecraft, airplanes, and many kinds of land and sea vehicles[3].

The type of oxidation that makes steel rust is not capable of harming aluminum.A layer of aluminum oxide about ten-millionths of an inch thick forms when oxygen interacts with the exposed metal surface, preventing further oxidation of the metal. In contrast to the rust that develops on iron, the aluminium oxide layer doesn't peel off to reveal a fresh surface that may also become oxidized. If the protective covering on the metal is damaged, It will instantly shut itself again.The colourless oxide layer is thin and securely attached to the metal underneath it. Aluminum is resistant to rust, corrosion, and flaking, unlike iron and steel [4].

Aluminum, when alloyed and handled correctly, can withstand corrosion from salt, water, and a host of other environmental factors, in addition to a wide range of physicochemical and chemical agents. Aluminum may be very reflective. Although anodized and dark anodized surfaces may absorb or reflect the light, electromagnetic waves ,radiant heat, and radiant energy, they are more effective in reflecting radiant energy. Because it is highly reflective over an extensive range of wavelengths, aluminum that has been polished is suitable for several functional applications.

1.1. ALUMINUM'S CHARACTERISTICS

Aluminum has a variety of unique qualities that have led to its extensive usage in a variety of applications and industrial processes, including:

- Due to its lower density than steel, aluminum is a lightweight metal.
- Alloys made of aluminum has a large strength to weight ratio.
- Due to its ability to maintain its strength at low temperatures, aluminum is frequently employed in cooling applications.
- Aluminum has a high wear resistance under typical operating conditions and does not develop coloured salts that stain neighbouring surfaces or taint things with which it comes in touch.
- Aluminum has a high degree of reflectivity and is a strong conductor of heat and electricity.
- Due to the absence of ferromagnetism, aluminum is a good substance to utilize in the electrical, electronic sectors.
- Because it does not show pyrophoric behaviour, it is a valuable material for applications involving the manipulation or Contact with flammable or explosive substances.
- Aluminum is safe for human consumption and is thus often used for food and beverage packaging. The natural finish of aluminum, which may seem glossy and smooth or brilliant and shining, is pleasing to the eye. It may be whatever colour or texture you choose.

• Aluminum is a recyclable material. The recycling market for aluminum is well-established and has a high scrap value, resulting in environmental and economic advantages.

• Simple to construct. All conventional metalworking and joining procedures may be used to shape and produce aluminum.

1.2. ALUMINUM ALLOYS

Its composition and microstructure influence aluminium alloy's mechanical, physical, and chemical properties. When pure aluminum is mixed with certain additional elements, its qualities and utility are significantly enhanced. As a result, most aluminum applications require alloys with one or more elemental additions. Copper, manganese, and silicon's most frequent alloying ingredients for aluminum are zinc and magnesium. For grain refinement and to produce special traits, additional components are added in smaller amounts. These elements are present in the alloy composition. In total number might be as high as 10%. (unless otherwise specified, percentages are expressed in weight%). Details of impurity are prevalent in aluminum alloys, although their overall proportion is generally less than 0.15 %. Cast composition and wrought composition are the two categories that make the most sense when dividing aluminum alloys into categories.

1.2.1. Wrought Alloy Families

The following is an example of a four-digit approach for generating a list of wrought alloy composition families:

•1xxx: Pure composition under strict control, employed mainly in the electrical and chemical sectors.

• 2xxx: The main component used to make these alloys is copper during the alloying process; nevertheless, the presence of other factors, such as magnesium, may be indicated. The remarkable strength of alloys in the 2xxx series, which can reach yield strengths of up to 455 MPa, has made them very popular in the aviation industry.

• 3xxx: Manganese-based alloys are used as universal in different products, such as those for architecture.

• 4xxx: Alloys in which silicon serves as the primary component of the alloying process; these alloys are often used in the production of welding rods and brazing sheets.

• 5xxx: These alloys include magnesium as their principal alloying component, and they are employed in the construction of objects associated with the sea, such as boat hulls and gangplanks.

• 6xxx: With silicon and magnesium as the primary alloying elements, silicon and magnesium-based alloys are commonly used in design casting and automobile components.

•7xxx: Alloys based on zinc are employed in the construction of aircraft structural components in addition to other high-strength applications.

• Alloys with the number 8xxx that are used to characterize different TiN, lithium, and iron compositions could make up a significant portion of the 8xxx series alloys, depending on the specific alloy.

• 9xxx: This number has been set aside for use at a later time.

1.2.2. Cast Alloy Families

The definition of casting compositions uses a three-digit method, followed by a decimal number. In each given situation, the decimal indicates the constraints that apply to casting alloys. After melting and processing, the decimals indicate the nuggets with the compositions. one and. Two should provide chemistries suitable for casting, as specified by the specifications. Casting compositions may be made using alloys from the following families:

- 1xx.x: Compositions that are unalloyed (pure). Under strict control, notably for making rotors.
- 2xx.x: alloys where copper serves as the main alloying component. There may be mention of other alloying elements.
- 3xx.x: alloys where a primary alloying component is a silicon. Different alloying elements like copper and magnesium are listed. Nearly 90% of all shaped castings are from the 3xx.x series.
- 4xx.x: The main alloying ingredient in these alloys is silicon.
- 5xx.x: The primary alloying agent is magnesiumin these alloys.
- 6xx.x: no use at the moment.
- 7xx.x: The major alloying component is zinc in these alloys. Additional alloying components you can pick between copper and magnesium.
- 8xx.x: The primary component of an alloy is TiNin these alloys.
- 9xx.x: Unused.

1.3. COMPOSITE MATERIALS

Light alloys have been used to make structural components in recent years due to a rising need for low-weight, high-performance structural materials for use in different industrial applications, as well as the urgent need to minimize emissions and fuel consumption in air and road transport. Due to their great moldability, outstanding

mechanical characteristics, and high thermal conductivity, a few of these elements, such aluminum-magnesium composites, are highly appealing for the fabrication of complex-shaped components. Despite this, the mechanical characteristics of these alloys deteriorate at temperatures below 200 °C, significantly restricting their usage is crucial aerospace and automotive components [6, 7]. A solid reinforcing phase, such as carbon or ceramic, must be added to produce Matrix Metal Compounds. It was created to combine the metal matrix's high strength, flexibility, and toughness with the reinforcing material's toughness [8]. The fact that reinforcement with particles retains the behaviour of the characteristics and allows for a considerable augmentation of mechanical properties in the most straightforward manufacturing techniques with the potential of applying secondary processes is one of the advantages of reinforcement with particles (forming, machining, welding)[8,10, 11,12, 13].

Composites are multiphase materials created by combining several elements to get qualities the individual components cannot achieve on their own [14]. The matrix (polymers, metals, or ceramics) is embedded in the composite material, and reinforcement (fibres, particles, flakes, and fillers) is embedded in it [15]. Figure(1.1) classifies composites.

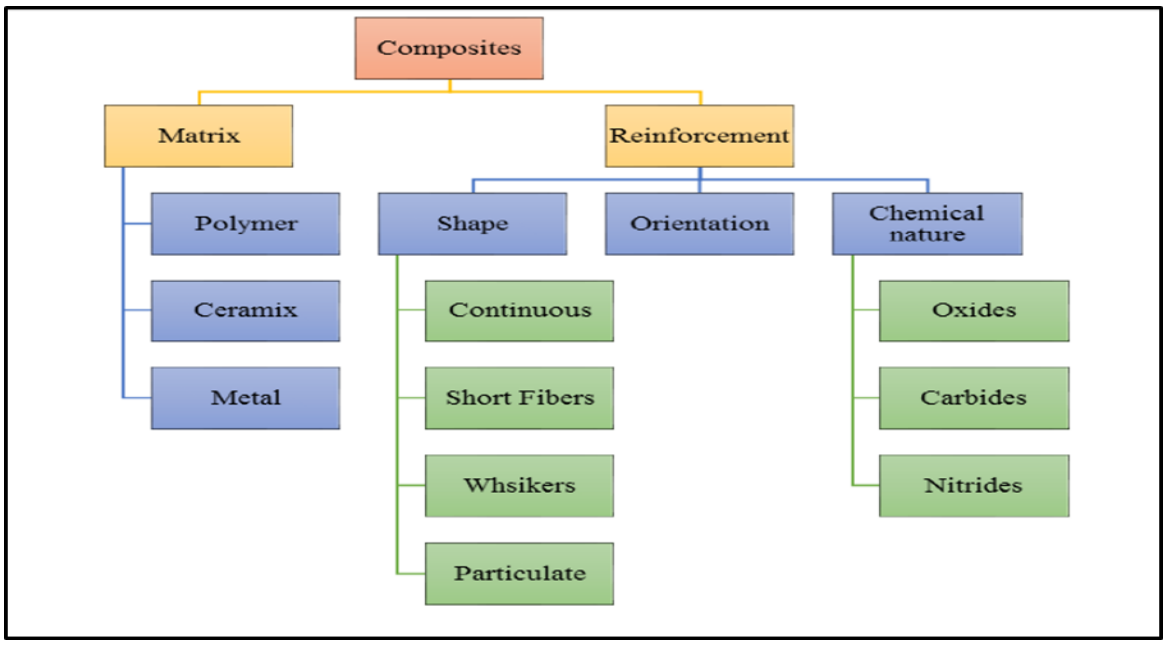

Figure 1.1. Classifies composites [16].

1.3.1. Metal Matrix Composites

Composites with a metal matrix, or MMCs, have at least two physically and chemically different phases that make up their composition. These phases are dispersed throughout the composite in such a manner that it has qualities neither of the steps could provide on its own. In most cases, one of the two phases is a fibre or particle phase that is dispersed across a metallic matrix.Other examples include: For instance, cutting tools and inserts for oil drilling, the aerospace and automotive sectors and heat control may use SiO_2nanoparticle enhanced Al nanocomposite [17].These are some of the benefits of MMCs:

- It saved a lot of weight because it was more vital for how much it weighed.
- Higher stability at high temperatures, creep resistance (compare SiO_2/Al to Al, for example).
- Improved cyclic fatigue characteristics by a lot.

Because MMCs have good properties, they can be used to solve many engineering problems with materials. Figure (1.2) shows materials with composite properties. The automotive, marine and aerospace industries have been used to make parts like robotic arms, electrical contacts, nozzles, cutting tools, and other things [18].

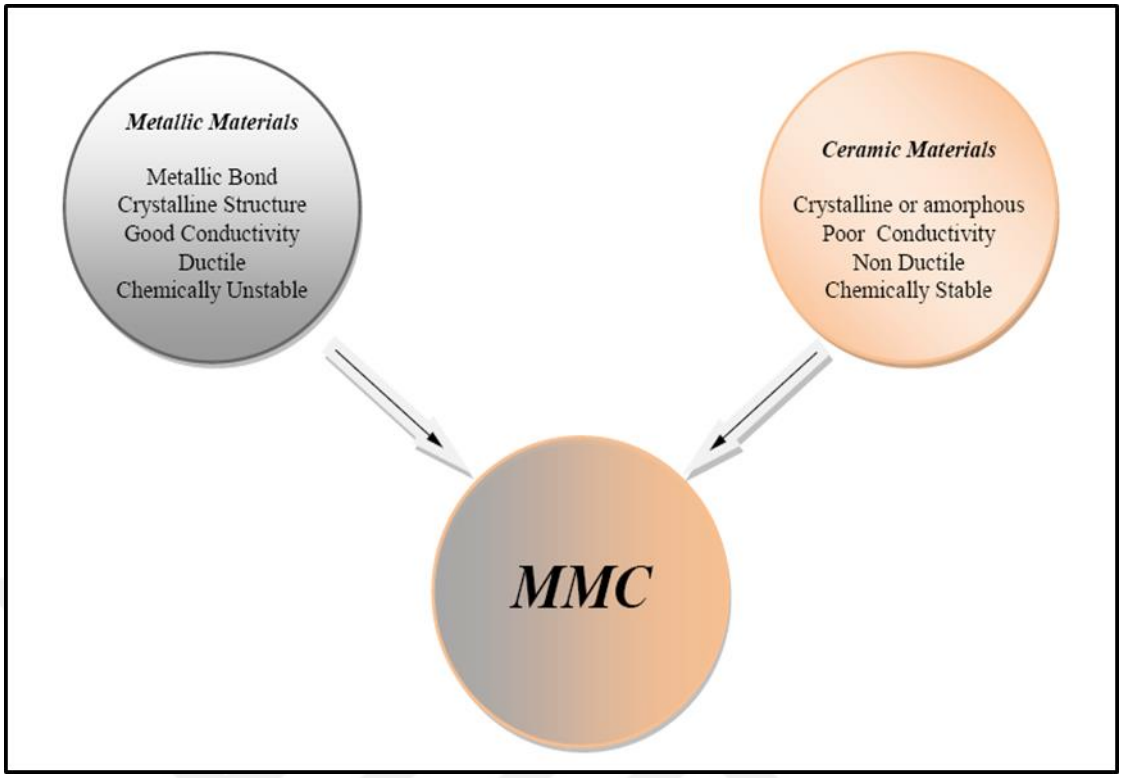

Figure 1.2. Shows the properties of the composite's parts.

As the "matrix," all matrix metal compounds are made of a metal or metal alloy. Metal or ceramic can be used as reinforcement. In very unusual circumstances, the composite may be constructed of a metal alloy that has been "reinforced" with a fibre-reinforced polymer matrix compound. One example of this composite is a glass-fibre-reinforced epoxy board, and another is an aramid-fibre-reinforced epoxy [18]. In general, metal matrix composites, often known as MMCs, may be broken down into three categories:

- MMCs that are reinforced with particles
- MMCs that are reinforced with short fibres or whiskers
- MMCs are supported with continuous fibres or sheets.

Figure 1.3 is a diagram of the three most common Metal matrix composites are classified as follows:

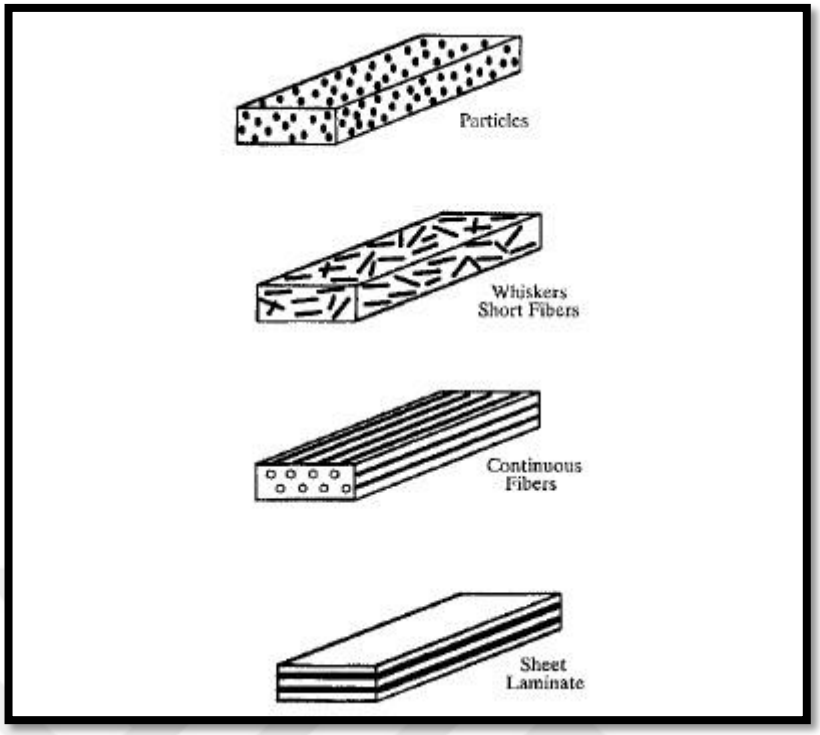

Figure 1.3. Composite metals of various types [18].

1.3.2. Composites Based On An Aluminum Matrix (AMC)

Due to its high strength, low density, toughness, plus resistance to corrosion, aluminum alloys are commonly employed in the aircraft industry. This is one of the main reasons why. Al-Mg–Cu and Al-Mg–Zn–Cu are unique precipitation-hardenable composites. Aluminum-lithium alloys can be precipitated to harden. Lithium increases aluminum's flexibility and density as the principal alloying element. This adjustment makes sense for the aircraft industry. Al-Li alloys can be precipitated like Al-Cu-Mg and Al-Zn-Mg-Cu. Al-Li precipitation hardening sequence, on the other hand, is much more complicated than in typical aluminum alloys that can be hardened by precipitation. These alloys usually have lithium, Titanium, copper, silicon, zirconium, and magnesium [19].

PART TWO

LITERATURE REVIEW

2.1. PRODUCTION ROUTES FOR NANOCOMPOSITES BASED ON ALUMINUM MATRIX

During manufacturing, the matrix may be in one of three states: melt, solid, or semisolid. This enables distinction based on the matrix's state. A rundown of the various manufacturing processes is shown below.

2.1.1. Processes In A Liquid State

Liquid state MMNC processing methods are suitable for producing near-net-shape components because they can be industrially scalable, inexpensive, and very easy [20]. This contrasts with other ways, which may be difficult, time-consuming, and costly. Liquid methods include techniques like an infiltration, stir casting, and ultrasonic-assisted casting.

Stir casting is among liquid-based technologies that are used the most often in the manufacturing of MMNCs since it is both simple and economical; it is suitable for application on large quantities of metals in general and aluminum in particular [21]. In most cases, the motor phase is introduced to the matrix before being mechanically stirred via the impeller to ensure that it is evenly distributed in the molten state. Through a process known as stir casting, particles of TiO_2 and SiO_2 were incorporated into aluminum matrices [22]. The basic form of the process is shown in Figure 2.1.

Ultrasound-assisted casting: how well ultrasound-assisted casting works to eliminate particle clusters caused by nanoparticle agglomeration propensity and poor wettability [24]. This refers to how well ultrasound-assisted casting works. It consists of ultrasonic melt treatment (typically frequency range of 18-20 kHz) when the boosting phase is added or after it has been added; The treatment was used to produce nanocomposites based on Al reinforced with Al_2O_3, B_4C,AlN, CNTs, and SiO_2 [25]. Ultrasonic melt treatment is a type of treatment that uses high-frequency sound waves to disrupt the molecular structure of the molten metal.

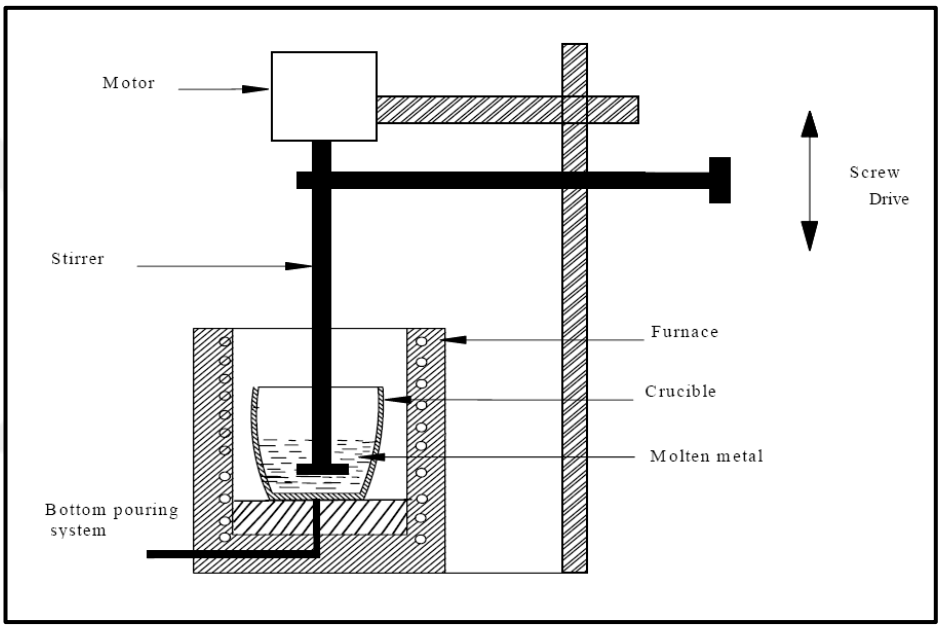

Figure 2.1. Stirring casting furnace which is used for purposes MMC [23].

Intrusion process: The injection of molten aluminum under stress into a porous structure is part of the leaching process. This technology has been widely adopted to produce composites with small-size reinforcement, for example, carbon carbide particles and TiC, foams, Al_4C3, Al_2O_3, AlN, and glass fibres [26].

2.1.2. Routes In Solid State

Powder metallurgy is the foundation for the solid-state procedures that are used in the manufacturing of bulk nanocomposites. When considering liquid and semisolid methods, the matrix and reinforcement wetting difficulties associated with nanoparticles are clearly and dramatically reduced [27]. The manufacturing of near-net-shape components is made possible by PM procedures, which are somewhat analogous to primary liquid and semisolid processing in certain respects. One of the competitive benefits provided by this processing approach is the ability to incorporate a greater volume proportion of reinforcement; another competitive advantage of this processing route is the possibility of creating matrix and reinforcement systems that are not possible to achieve using conventional liquid casting methods[28].

2.1.3. Semisolid State Methods

A partly solid mixture (slurry) moulding using relatively tiny grains close to globular at solid fractions ranging between 20 - 60 % is involved in semisolid casting. In general, semisolid procedures provide several benefits, the most notable of which areporosity, non-turbulent filling,low shrinkage, and a lower temperature throughout the processing stage. They can be separated into two primary categories of procedures: thixo-processes and rheo-processes (compocasting) [29].

.1.4. Hybrid And Other Methods

Aluminum nanocomposites may be manufactured by combining two or more techniques mentioned. Before the formation of the nanocomposite, these approaches often include the employment of processes that involve metal powder (liquid state or composite moulding methods). The micron or nano-sized metal powders of the

appropriate weight and size either method may be used to create master powders (1) Solid nanoparticles are mixed or blended. (2) Using a ball mill for mechanical alloying fused, in the melted [30]. The selective aluminum alloys of interest are the result of this preparation.

2.2. MECHANICAL BEHAVIOR OF Al-NANOCOMPOSITES

Mechanical behaviour for Al-based nanocomposites may be broken down into two primary sections, each offering a different perspective on the mechanical characteristics possessed by these compounds.

2.2.1. The Static Mechanical Properties At Room Temperature

Incorporating reinforced nanoparticles into alloy clues a general improvement in the material's mechanical characteristics compared to corresponding non-reinforced alloys, as in Figure 2.2.The improvement produced with micro-reinforcement at the same weight % is often superior.Notably, YS has significantly increased. The higher dislocation density is principally responsible for the differences in values between nanocomposites and the homogeneous aluminum matrix.Only a minor role in this process is played by direct loading by nanoparticles. [36]. The presence of nanoparticles is responsible for an increased work hardening rate, which contributes to the increased tensile strength [37].On the other hand, there is often a threshold size/weight reinforced fraction.Past that point, adding more nanoparticles causes a decrease in the material's mechanical properties [31, 33]. This behaviour is primarily caused by the increased presence of nanoparticle agglomerations and a higher degree of fine porosity [33], both of which decrease the composite's flow pressure. Additionally, Due to a mismatch in the thermal expansion coefficient between the matrix and the solid particles, high dislocation density and other defects near the solid particles might cause decoherence at the particle/matrix interface.

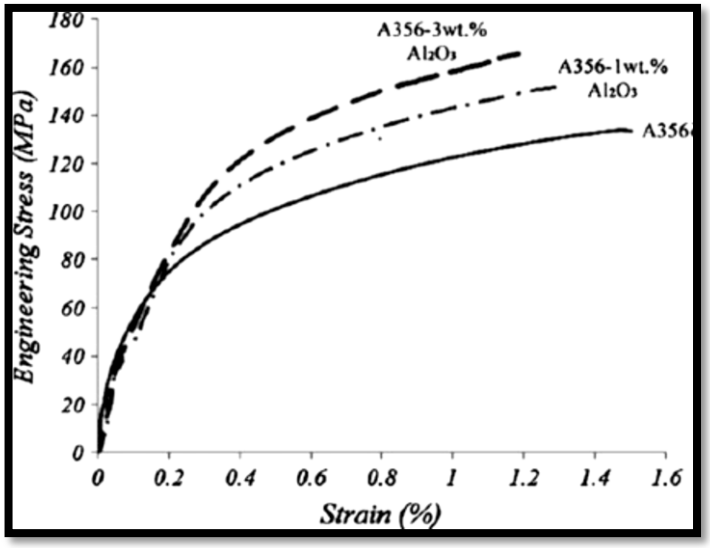

Figure 2.2. The stress-strain curves of hybrid nanocomposites by casting tensile under tensile strength [31].

The tensile properties (UTS, YS) as a function of fracture size in strengthening AL-based nanocomposites have been proven in various research [34, 37, 38]. These findings are depicted in the graphs displayed in Figures 2.3 and 2.4. the molten stir-moulding compounds achieved the maximum UTS between (2-3)%V of the reinforcement. On the other hand, the composites represented a steady directional increase of the UTS with increasing the volume fraction. This was the case despite the composites undergoing the main powder grinding before the stir casting. Without subjecting the material to heat treatment, the highest result of the researched information, around 303 MPa, may be reached for nanoparticle concentrations of up to 5% [37]. When different methods of casting are compared, it is frequently found that composite casting provides higher mechanical qualities than stir casting when the same matrix, kind of reinforcement, and volume/weight percentage are used [31]; the mechanics of basic stirring are improved by grinding combined support with metal powder before stir casting [34]. These findings are based on the assumption that the matrix, type of reinforcement, and volume/weight fraction are the same.

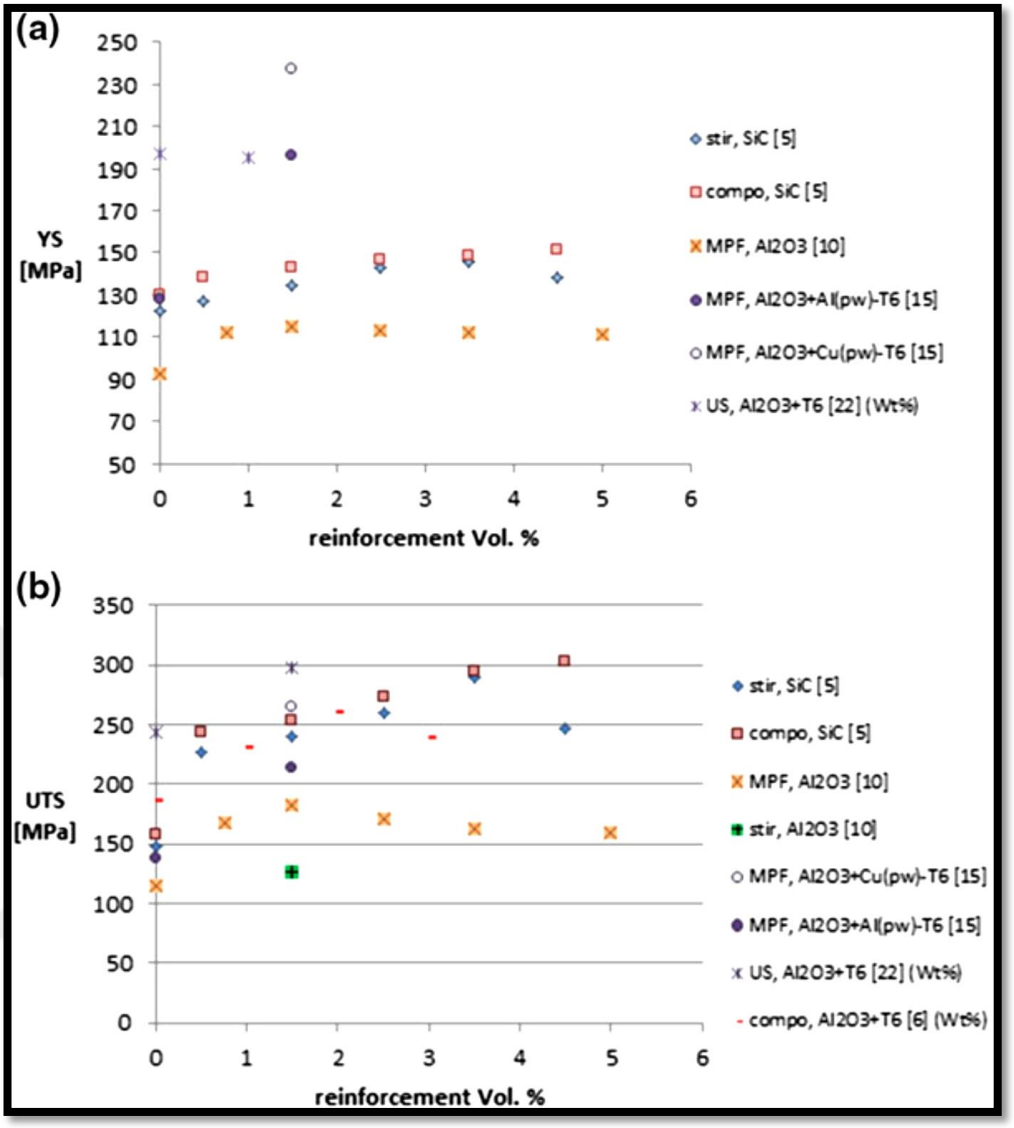

Figure 2.3. YS (a) and UTS (b) for asl-based nanocomposites with varied manufacturing processes and reinforcement.

.

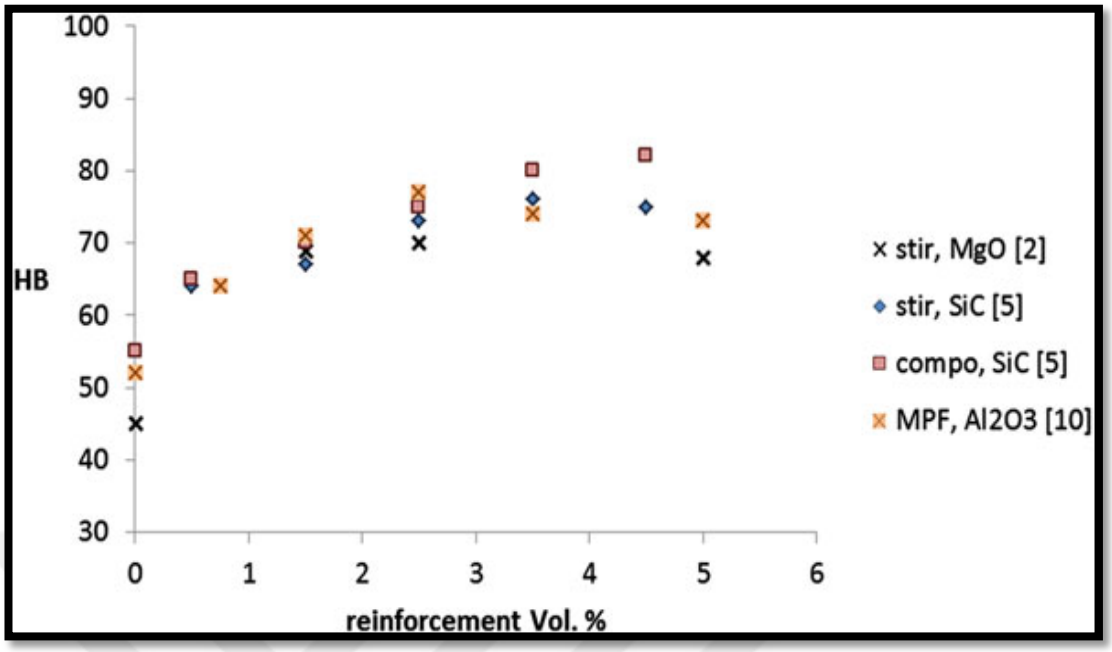

Figure 2.4. The function of volume % for al-based nanocomposites manufactured using various methods and reinforcements.

It should be noted that casting at 800 °C increased compressive strength up to 5 %vol of the nanoparticles strengthening. Still, the maximum compressive strength was reached while throwing at 850 °C with 1.5 %vol of the nano components. Secondary operations, such as hot extrusion, may control or alleviate the harmful effects of porosity [33, 39]. As found in the Al6061-Al_2O_3 composites [33],By raising the weight fraction of the reinforcement near to 1% in the casting condition, the mixes' UTS, YS, and hardness were all enhanced,after that eroded as a result of the high porosity content and the uneven distribution of nanoparticles. Generally, The hot extrusion procedure enabled a continuous increase in the mechanical properties further than limiting weight fraction thanks to a decrease in porosity, a more uniform distribution of nanoparticles, and an improvement in the interconnection between particles and the matrix microscopic condensation, and a more uniform distribution of nanoparticles. 1.5 wt % hot extruded nanocomposites demonstrated a near doubling of Y.S. and UTS compared to the unsupported hot extruded materials. Adding ceramic nanoparticles often results in grain refinement [34, 40]. Therefore, it

is crucial to determine if the strengthening of the nanoparticles is a direct or indirect impact on the microstructural improvement generated by the nanoparticles.

2.2.2. Mechanical Properties At High-Temperature

Very little information is currently known for those interested in the mechanical properties of Al-based nanocomposites produced via fluid channels at high temperatures. [41].This was found to be the case. In particular, the addition of 2 % vol. Additionally, churning a semisolid sludge with a 30% solid fraction produced nanocomposites that could maintain 90% of YS under 300 °C (142 MPa) as opposed to ambient temperature (158 MPa).However, The non - reinforced alloy produced with the identical casting method showed YS of 79 MPa at 300 °C (60 % of the room temperature value).The aluminium matrix's creep resistance is improved by including incoherent, non-shearable second-stage nanoparticles by preventing climbing or sliding processes from occurring or bearing a heavier load than the matrix alone. [42, 43], as is the case with fine particles of oxide or carbide [44]. It is expected that the use of particles of smaller sizes will enhance the creep resistance due to the shorter inter-particle spacing. At the same time, the more rigid reinforcement may be able to withstand higher pressure [45]. It was shown that there is a shift in creep behaviour with the transition from a static to a sliding substructure model.This happens when the temperature reaches a critical point better than Al-based composites supplemented with micrometre ceramic particles [46].Because the disturbances and stresses needed for micrometric reinforcing particles are too tiny to be considered in the threshold stress computation [47],it is possible to conclude that nanoparticles are more effective than micrometric particles in stabilizing disturbances.

2.3. WEAR

When two surfaces rub against one another, they eventually wear away some of the material on both of them. This phenomenon is known as wear. Two popular types of clothing that people wear are:

- Adhesive Wear
- Abrasive Wear

Scouring, galling, and seizing are some other names for adhesive wear. The primary mechanism behind adhesive wear is a deformation that occurs during shear. In most cases, significant contact stresses cause local plastic deformation, ultimately creating adhesive connections between the two surfaces, as in Figure 2.5. Continued use of the sliding motion will result in a rise in the shear stress inside the bonded area [48]; this will continue until a material's yield strength is significantly exceeded.

As shown in Figure 2.5, the buildup of solid ceramic nanoparticles, like TiO_2 or SiO_2, among sliding surfaces leads to the development of abrasive wear.The quantity of material lost depends on how hard the sliding surface and ceramic particles are (either in volume or mass).An additional influence in wear is sometimes the surrounding environment. Fretting, cavitation, erosion, and other problems may result from it. The contact regions mate when surface asperities are gradually smoothed down by abrasive wear. As a result, the local contact stress is reduced as a direct result of the expansion of the contact area. After the surface has been first worn down by abrasion, the oxidized particles begin to be removed from the surface. Because it needs the denuded surface's reoxidation to continue removing oxidized particles, this is often a process that takes place in a constant state. If the contact pressure is strong enough to shear the particles, the final wear step takes place in the adhesive mode. This stage takes place in an adhesive way. The action of shearing causes the development of thin wear debris sheets in the shape of plates. The sheets may result in a large amount of material loss. However, this is contingent on the applied stress [48].

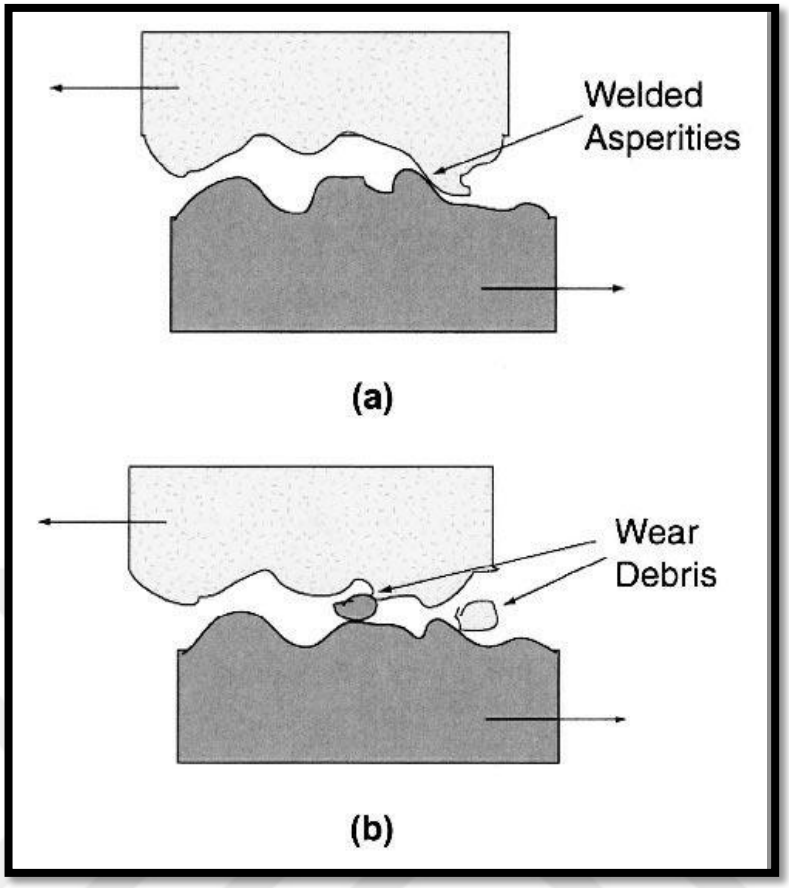

Figure 2.5. Adhesive wear results from high contact stresses (a) the intensity of welded and (b) two surfaces that wear debris. [48].

It is essential to keep in mind that wear is, in the vast majority of cases, a feature of the system. Consider the many different variables at play here, including the matrix, the reinforcement fibres or particles, the orientation of the threads with the direction of wear,the volume fraction, the reinforcement interfaces,and the size,and morphology, of the compound. At the microscopic level, they are the intrinsic variables. The circumstances of the test or the operation might also impact the wear behaviour. These factors contain the nature of the abrasive or counter surface, the force used, the pace at which it is applied, the geometry,the contact area, and the surroundings (dryor lubrication). These are considered to be outside factors. The inset describes two effective methods for determining whether or not corrosion has occurred. When the circumstances are appropriate, incorporating ceramic particles into a metal matrix may increase the material's resistance to wear. On the other hand, one must be aware that the inclusion of ceramic particles may lower the wear

resistance if the circumstances are not optimal. This is something that must be taken into consideration. For instance, It is possible to remove ceramic particles from the matrix, causing three abrasive materials to erode into the body, causing a corrosive process,as shown in figure 2.6. (b). Another thing to remember is that the size of the fracture or the size of the reinforcement becoming massive causes the fracture to get larger. It is anticipated that the material's hardness would be significantly diminished. The particles will fracture if the hardness of the fracture is not enough. Contributing to erosion. This challenge aims to increase wear resistance without sacrificing the product's durability [49].

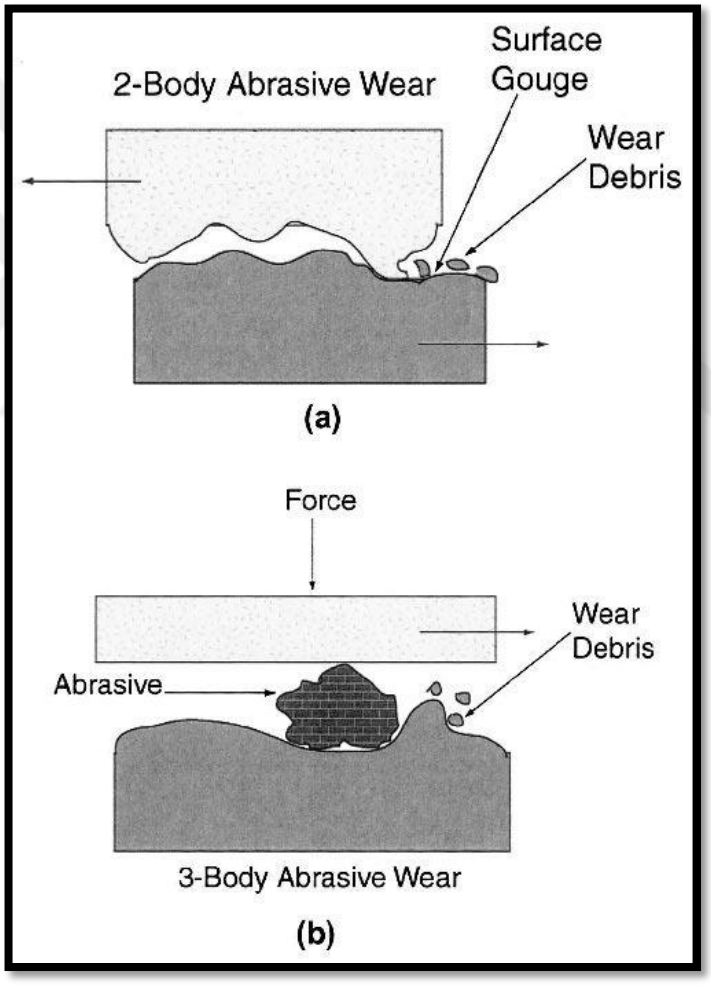

Figure 2.6. Two-body erosion (a) and triple-body erosion (b) are two types of abrasive wear that involve ceramic particles and cause debris to get stuck between surfaces that slide. [48].

2.3.1. Wear In Aluminum Matrix Composites

MMC wear is now in its abrasive phase; the amount of wear is influenced by the applied load, velocity, volume, volume %, and binding strength of the reinforcement to the matrix. [50 , 51]. When ceramic particles, like alumina, are added to aluminum alloys, the wear rate decreases significantly [52]. The size of the reinforcement particle and the amount of reinforcement in the material determine how much the wear rate slows down. Most of the time, According to Fig. 2.7, the alloy with the largest size of particles and volume fraction has the best wear resistance.Figure 2.8 displays how SiO_2 particles can affect wear resistance [53]. The composite performs better than the unreinforced alloy under a higher load.

The surface of unreinforced aluminum alloys worn down usually has long, continuous grooves. This is because abrasive particles have been ploughing the surface. On the other hand, there is much less surface pushing on the surface of composites [51]. Composites' rate of wear lowers as the reinforcing volume fraction increases.When particle size increases, the wear rate usually goes down. This may be because particle strength is better for smaller particles than interface strength.So, The more significant parts can carry the loadon the surface and remain in the matrix for longeruntil they break into smaller pieces.

The fracture toughness of reinforcement is just as important as how hard it is. As the stress increases, the reinforcement's ability to break becomes an important parameter. How much the support will break depends on how hard it is to die. So, the toughness of the particles that make up the reinforcement is what controls wear as stress goes up.

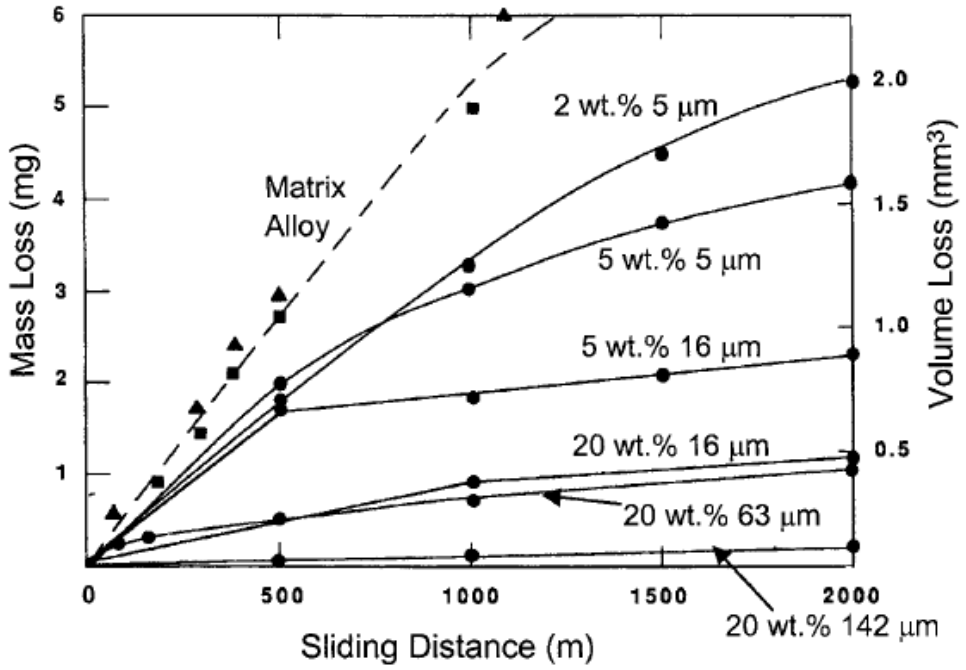

Figure 2.7. The wear resistance of aluminum alloy matrix composites gets better as the size of the particles gets more extensive and more particles are added [52].

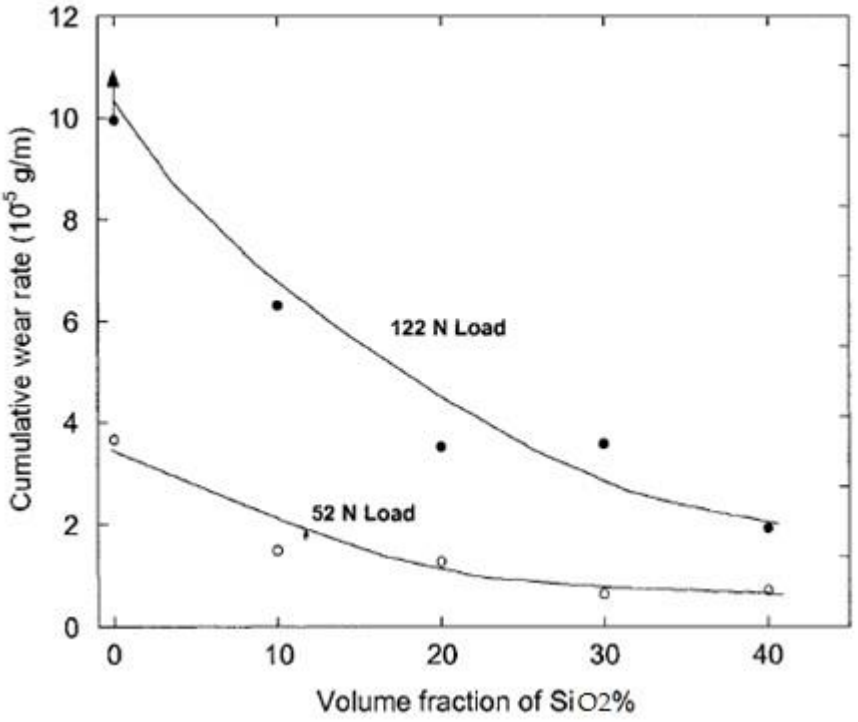

Figure 2.8. Wear resistance increases with the growing fracture size of SiO_2 [54].

Most of the time, By using a lubricant or reinforcement with lubricating characteristics, you can also improve wear performance.Carbon from aluminum graphite particles can lower the friction coefficient against dry steel [55]. On the other hand, microcrystalline carbon didn't do much of anything. This makes sense because graphite flakes easily break and work as a lubricant. The wear rate can be significantly affected by the surrounding environment.

2.4 WETTABILITY

Wettability means that On a solid surface, a liquid can disperse. It measures how close a solid and a liquid are to each other. The melt must wet the solid ceramic phase for solid ceramic particles to be successfully poured into a mould [56]. For MMC's composites to be processed, The liquid metal must wet the ceramic phase.For the infiltration and hardening of the material to occur, Contact between the liquid matrix, metal, or alloy and the reinforcing material (fibres, particles)is required. The amount of wetness in the metal on the reinforcing material will determine the percentage of liquid metal that goes into the moulding.The contact angle shows how moist a character is, which is created when a drop of liquid sits on a solid surface.This is shown in Figure 2.9. Following equation demonstrates the relationship between the surface force vectors:

$$\gamma_{SV} - \gamma_{SL} = ¼\ \gamma_{LV}\ \text{Cos}\ \theta \qquad (2.1)$$

The solid-liquid, solid-vapour and liquid-vapour interfaces surface energies are γ_{SV}, γ_{SL}, and γ_{LV}.Young's equation is the connection in Eq. (2.1), and Gibbs later validated it using thermodynamics. [57].

Because many manufacturing processes include a liquid phase of metal that comes into touch with solid ceramics at some point throughout the process [59], The wettability behaviour of molten metals on a solid substrate has become more

important in developing metal-ceramic composites. Figure 2.9 shows how the contact angle between the molten metal and the ceramic affects the degree of wettability. When the angle is less than ninety degrees, wetting will occur. Suppose that intermolecular cohesion is stronger than liquid molecules on a solid's surface. In this scenario, the liquid will not wet the liquid, according to Fig. 2.10a. In the example, there is better adhesion between the ceramic wall and the liquid particles shown in Fig. 2.10b.This leads to increased capillarity and, thus, superior wettability.

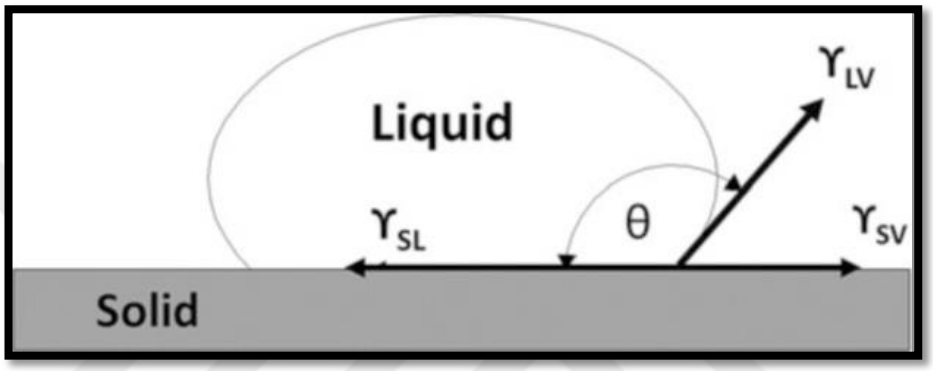

Figure 2.9. The surface forces act at the point where a liquid and a solid meet [58].

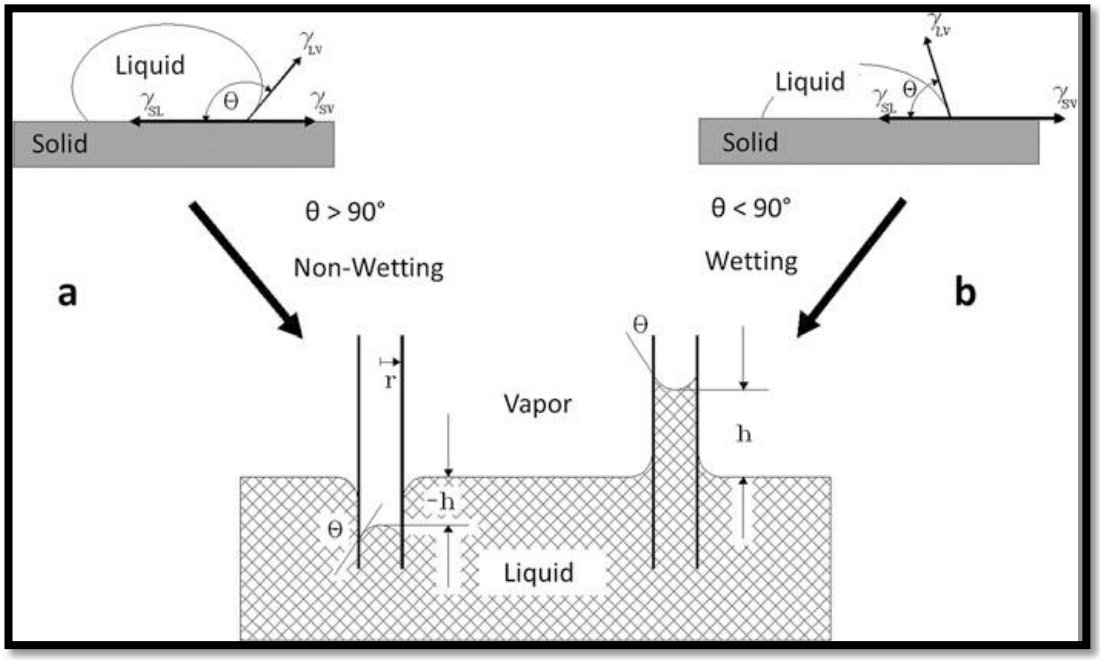

Figure 2.10. (a): System that doesn't get wet. (b) The humidification system is based on the contact angle [58].

PART THREE

MATERIAL AND DEVICES

Through this work, the researcher will add different weight ratio of TiO_2 and SiO_2 nanoparticlesand study their effect on themechanical properties and wear resistance of aluminum alloys and compare them. Composite materials containing different proportions of TiO2 and SiO2 was cast by stirring method. The microstructure and phases will be verified through the use of optical microscopy, SEM and X-ray diffraction. The tensile and hardness test is used to study the effect of adding reinforcement on the mechanical properties. It will study the wear rate using a wear test pin on a disk device for both the basic Al alloy and the hybrid composite under different loads (5, 10, 15) N and at a sliding speed of (2.8) m/sec using different times (5, 10 and 15) min.

3.1. MATERIALS

Al6061 alloy used in this work as the matrix material was purchased from local markets produced by a Liande metal supplier. And it is in the form of plates, where we cut it into a small cat as in the figure (3.1) so that we can put it in the pudding and melt it in the stirring furnace.

Figure 3.1. Al 6061 alloy.

The two tipnanoparticles (TiO_2 and SiO_2) used in the studyas the hybrid reinforcements were purchased from local markets and produced by Hongwu Nanomaterial Group Ltd. As shown in Figure (3.2), the purity of TiO_2 is 99.9 %, its particle size is 30 - 50 nm, the purity of SiO_2 is 99.8 %, and its particle size is 20-30 nm.

(a)

(b)

Figure 3.2. Appearance of (a) TiO_2 and (b) SiO_2 nanoparticales.

The pure magnesium (Mg) element, also purchased from the local markets, is in the form of a strip, It was used to improve the alloy's wettability as in the Figure. (3.3).

Figure 3.3. Pure magnesium (Mg)

3.2. MAIN DEVICES

Several tools and devices were used in this studyfor preparation and characterization of the composite . In the section, the information abut these test instruments is given below. Note that all the devices used by the researcher are in the Department of Production and Metallurgy Engineering , Nanotechnology laboratories and the Advanced Materials Research Center at the University of Technology, Baghdad.

3.2.1. Stir Casting Furnace

This furnace was used to melt aluminum alloy and melt the added magnesium, then mix the resulting molten with nanopowders that are added in different weight ratios, according to Figure (3.4).

Figure 3.4. Stir casting furnace [23].

3.2.2. Sensitive Balance (Type Denver Instrument)

Sensitive Balance was Use to calculate the weight of the aluminum alloy, the pure magnesium element, and the Nanopowders, as shown in Figure (3.5).

Figure 3.5. Sensitive balance.

3.2.3. Stainless Steel Mould

For the purpose of obtaining samples, the molten metal is poured into the mould. In the cylindrical shape with main dimensions (diameter = 15 mm and height = 150 mm) to conduct tests on them, as in Figures (3.6) and (3.7).

Figure 3.6. Stainless steel mould.

Figure 3.7. Stainless steel mould.

3.2.4. Convection Oven

This furnace is used for heating magnesium and Nanopowder before adding it to the molten aluminum, in addition to heating the mould before pouring the molten into it, as in Figure (3.8).

Figure 3.8. Convection oven.

3.2.5. Turning Machine

Machine-type Knuth tools are used to cut, run and prepare samples for subsequent examinations, as shown in Fig. (3.9).

Figure 3.9. Turning Machine.

3.2.6. Grinder AndPolishing Machine Model DAP-5

We used this device to clean the samples using different SiC papers and water, polishing them and preparing them for wear, Optical microstructure, and X-ray scanning, as seen in the following Figure (3.10).

Figure 3.10. Grinder and polishing machine.

3.2.7. Microstructure Examination Device

The prepared samples were examined using a metallographic microscope with the help of a digital optical camera model (A. Kruss Opronic), as shown in Figure (3.11) to study the microstructure.

Figure 13.11. Optical microstructure.

3.2.8. Tensile Test Machine

The tensile testing was conducted using an Instron machine (DWD-200E), as seen in Figure (3.12).

Figure 3.12. Tensile test device.

3.2.9. Wear Test Equipment(Pin On Disc)

A wear device (pin to disc) local industry in Iraq performs the wear test., Figure (3.13). This device consists of a disk rotating, a sample holder, And motor that rotates at a constant speed of (490 rpm), and the disk has a roughness of 1.9 μm and a

H.V = 217.the sample is then subjected to loads that are perpendicular to it. Atmospheric pressure and room temperature were used for the testing of dry wear.

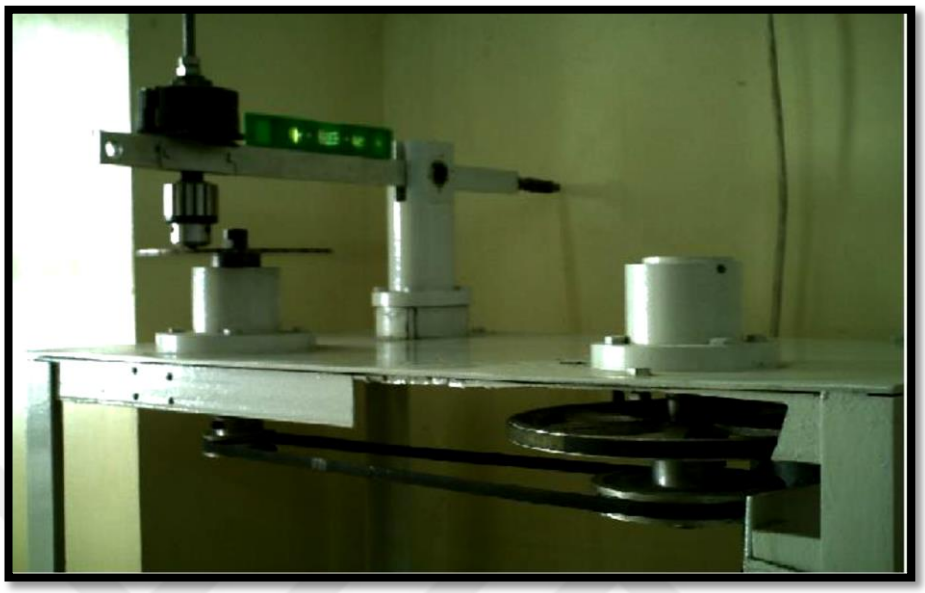

Figure 3.13. Pin on disc device.

3.2.10. X-Ray Diffraction Test Device

The X-ray diffraction test was started to detect the phases created by the primary matrix alloy and the composites. The brand of the test machine is Shimadzu-6000XRD as indicated in Figure (3.14).

Figure 3.14. X-ray diffraction test device.

3.2.11. Scanning Electron Microscopy (SEM)Device

A VEGA 3 L.M. type electron microscope produced by TESCAN, a Czech Republic company, contained in an Energy Dispersive Spectrometry (EDS) detector (MAX3 model from Oxford British company) was used to obtain the exact chemical composition associated with SEM as seen in Figure (3.15).

Figure 3.15. SEM device.

3.2.12. Hardness Test Device

Vickers digital hardness instrument TH714 was used for the testing, as seen in Figure (3.16).

Figure 3.16. Vickers digital hardness device.

PART FOUR

METHODOLOGY

4.1. PREPARATION OF COMPOSITE

We have used 6061 aluminum alloyas the matrix material manufactured by Hongwu Nanomaterial Group Ltd. The findings of our chemical investigation of the alloy are shown in Table (4.1) below.

An electric furnace heated to 800 C° was used to melt the Al 6061 alloy, which was then poured into a 300 C°-heated steel mold, cylindrical shape with dimensions of (diameter = 15 mm and height=150 mm), Figure (3.6) in part (3) showed the mould.

Table 4.1. Al 6061 alloy chemical analysis.

Al	Si	Cu	Mg	Zn	Mn	Ti	Cr	Zr	Fe
97.5	0.674	0.227	0.879	0.015	0.15	0.0541	0.133	0.002	0.704

The production of composites was based on the stir casting method, wherein an electric furnace heated to 800 °C melted the matrix alloy.The melt was maintained at this temperature for 15 minutes to homogenise the chemical composition.Then, Mg (1 wt %) was added to increase wettability, and reinforcments (silicon dioxide and titanium dioxide) were gradually added to the melting alloy using stirring. mechanical, weight fractions of the addedTiO_2:SiO_2 particles were 0.1:0, 0:0.1, 0.1:0.1, 0.3:0, 0:0.3, 0.3:0.3, 0.5:0, 0:0.5, 0.5:0.5, 0.1:0.3, 0.1:0.5, 0.3 :0.1, 0.3:0.5, 0.5:0.1 and 0.5:0.3 wt%, which were preserved with aluminum foil and heated up to 300°C for 1 hour (to help improve the wettability and solubility to reduce moisture) after melting inside the vortex by an electric motor at a speed of rotation (750 rpm) for excellent dispersion of the arms within the melt. To create the composite material reinfoced by SiO_2 and/or TiO_2 nanoparticles, the molten mixture is then put into a

heated mold, whose properties will be mentioned in Table (4.2). The process was repeated for all the above additions.

Table 4.2. Characteristic of Nanoparticles powder (TiO_2 and SiO_2).

Characteristic	**Nano TiO_2**	**Nano SiO2**
Manufacturer	Hongwu International Group Ltd,	Hongwu International Group Ltd,
Appearance	White powder	White powder
Purity	99.9%,	99.8%
Grain size (nm)	30-50 nm	20-30 nm
Bulk density (g/cm3)	4.23	2.66
Melting point (^oC)	1843	1782

4.2. TESTS AND EXAMINATIONS

4.2.1. The Optical Microstructure Examination

6061 aluminum alloys and samples of SiO_2 and/or TiO_2 composites dietilled were cut to dimensions (15 × 10 mm). To remove the oxide and/or heterogenic layer, samples were prepared using a grinding machine with fine carbide paper (400, 600, 800, 1000, 1200). The pieces were then polished with a polishing cloth and alumina (5 μm) to remove the grinding damage.

After polishing and grinding were completed, After cleaning the samples with the water and alcohol, the surfaces were exposed to an etching solution (3%H.F and 97 % water) for 10 seconds to reveal the grains and features.It was then washed with water and alcohol before drying with hot air.Samples were tested using a metallographic microscope with the help of a digital optical camera model (A. Kruss Opronic).

4.2.2. Test Of Hardness

Vickers digital hardness tests on the primary Al 6061 alloy and the composites were performed using the TH714 model of the Vickers hardness tester, prepared for microstructural testing without etching. For a period of rest, a load of (200 g) is used (15 seconds). The average hardness value was calculated using three measurements for each sample. Here is the equation for calculating Vickers hardness in HV0.2[63]:

$HV = 1.8544 * P/(dav)^2$ (4.1)

HV: Vickers hardness f(kg/mm2)

P**:** applied load (kg.f)

dav**:** diagonal length (mm)

The hardness tested Al 6061 alloy and composites results are displayed in the table (4.3).

Table 4.3. Hardness rate for samples.

Vickers Hardness (HV0.2)		% Weight Fraction of TiO_2			
		0	0.1	0.3	0.5
% Weight Fraction of SiO_2	0	68.88	74.57	75.76	79.17
	0.1	71.38	76.05	76.25	84.42
	0.3	73.31	77.35	86.68	86.03
	0.5	75.91	86.96	85.89	94.87

4.2.3. Tensile Test

The tensile test was performed on the samples after they had been produced under the (ASTM E8) standard, as illustrated in Figure (4.1). The tensile test was carried out using the Instron apparatus (DWD-200E). Table (4.4) shows the test findings up to the fracture stage, as seen in Figure (4.2).

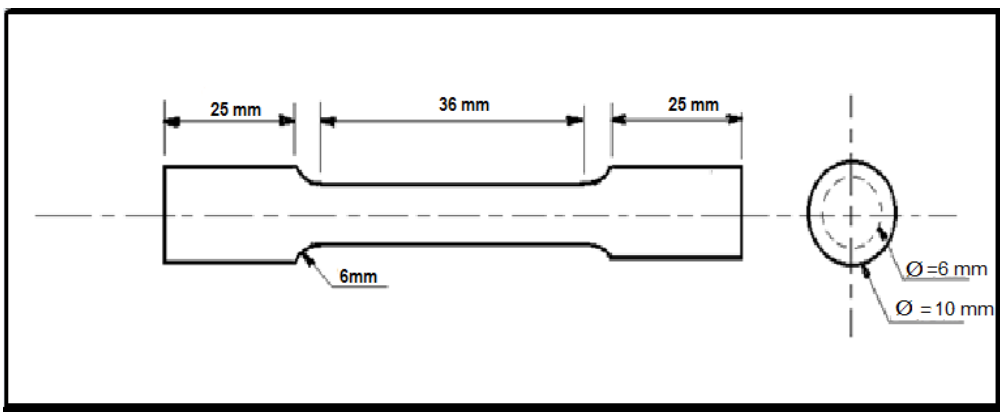

Figure 4.1. Standard tensile test specimen.

Figure 4.2. Samples after tensile test.

Table 4.4.Yield strength (YS) MPa, Ultimate tensile strength (UTS) MPa, and elongation (Ę) % of base alloy and composites

Ultimate Tensile Strenght (MPa)		% Weight Fraction of TiO_2			
		0	0.1	0.3	0.5
% Weight Fraction of SiO_2	0	36.24	62.19	69.11	79.12
	0.1	55.20	79.38	87.48	105.25
	0.3	64.65	87.25	96.76	145.41
	0.5	77.10	90.17	110.50	151.12

Yield Strenght (MPa)		% Weight Fraction of TiO_2			
		0	0.1	0.3	0.5
% Weight Fraction of SiO_2	0	34.92	46.37	52.91	53.44
	0.1	48.80	35.87	66.12	69.05
	0.3	56.22	65.37	68.33	70.68
	0.5	71.87	72.68	70.42	76.87

Elongation (%)		% Weight Fraction of TiO_2			
		0	0.1	0.3	0.5
% Weight Fraction of SiO_2	0	31.39	22.85	17.95	14.15
	0.1	29.85	17.09	13.84	13.15
	0.3	21.42	14.35	11.60	11.36
	0.5	14.95	12.61	11.49	9.61

4.2.4. X-Ray Diffraction

In order to determine the resultant phases of Basel alloys and composites, an X-ray diffraction test was conducted using an apparatus of type (Shimadzu- 6000XRD)

under the conditions of a copper target (current = 30 mA). (voltage = 40 kV) and a small range (20-80) degrees.The results of the analysis of the nanoparticles powder for each TiO_2 and SiO_2 were as shown in the following figures and tables:

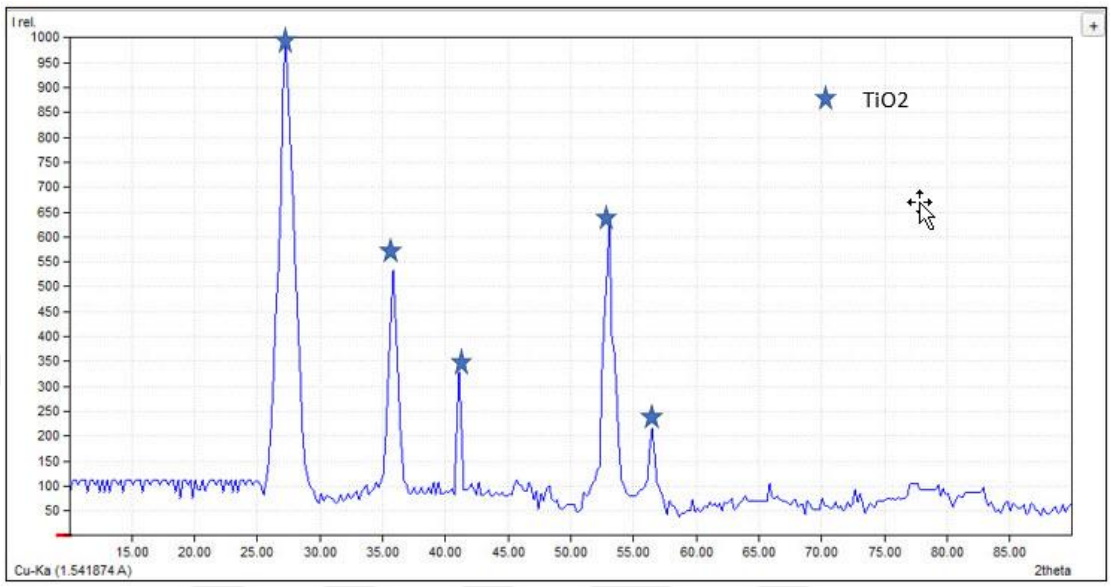

Figure 4.3. X-ray diffraction analysis for tio_2 nanoparticles powder.

Θ standard	**Θ measured**	**(h k l)**	**Int standard**
27.446˚	27.38	(1 1 0)	100
36.085˚	35.90	(1 0 1)	50
41.225˚	41.13	(1 1 1)	25
54.322˚	53.80	(21 1)	60
56.640˚	56.94	(2 20)	20

Table 4.5. Result of XRD examination for TiO_2 nanoparticles powder.

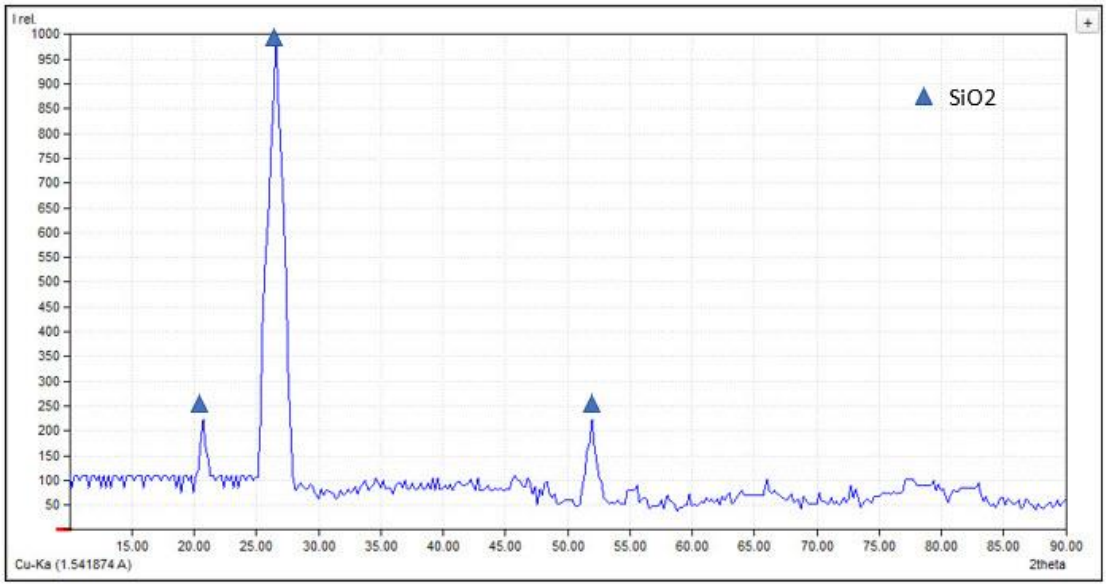

Figure 4.4. X-ray diffraction analysis for SiO_2 nanoparticles powder.

Θ standard	Θ measured	(h k l)	Int standard
20.860˚	20.90	(100)	16
26.639˚	26.59	(101)	100
50.138˚	51.98	(112)	13

Table 4.6. Result of XRD examination for SiO_2 nanoparticles powder.

4.2.5. SEM Test

A scanning electron microscope (VEGA 3 L.M.) was produced by TESCAN, a company in the Czech Republic; It was used to study the topography of the reinforcements and samples. Energy dispersal spectrometry (EDS) detector (MAX3 model from Oxford British company) was used to obtain the exact chemical composition associated with SEM.

4.2.6. Wear Test

After obtaining samples with dimensions (15 mm) diameter and (150 mm)high from the base metal and composites, they were shaped in a lathe machine to get samples for wear test with dimensions (10 mm) diameter and (20 mm) high and then prepared by continuously milling SiC paper (400, 600, 800, and 1000), Diamond paste is then used for polishing. Before being dried in hot air, the samples are washed with water and alcohol.The wear device's wear test is carried out by the domestic industry (pin to disc), as mentioned in the third part. This device consists of a disk rotating and a sample holder;the device has a motor that rotates at a constant speed of (490 rpm), and the disk made of carburized steel has a roughness of 1.9 μm and an H.V= 217. the sample is then subjected to loads that are perpendicular to it. Atmospheric pressure and room temperature were used for the testing of dry wear.

The following information has been used to determine sliding distance [64] :

$$SD = 2\pi rnt \quad (4.2)$$

SD: Slidingdistance (cm)

r: The distance between the specimen's and the disc's respective centres (cm)

n: The disc's rotational speed (490 r.p.m)

t: Time (min).

The Following Equation Determines The Sliding Speed [64]:

$$V= 2\pi rn/1000 \text{ x}60 \quad (4.3)$$

V : Velocity (m/sec)

The weighting technique measures the wear rate. Weighting the samples before and after the tests with a digital balance with an accuracy of up to (±0.0001 g) allows for calculating changes in the relative mass. Loads of (5N,10 N and 15 N) were used with speeds of sliding (2.8 m / sec) and times of (5, 10 and 15) min. After each test, the disc was polished and cleaned.The following methods were used to gauge the rate of wear [64]:

Wear rate = $\Delta w / SD$ (g/cm) (4.4)

ΔW: The Specimen's Weight Before And After The Test (g)

SD: Distance Of Sliding (cm)

The experiment's foundation was chosen using the wear and tear metrics, and composite alloys were: load (N) and time (min). Each variable has three levels listed in Table (4.5) and a constant sliding velocity (m/s), and this process are repeated for all samples.The results of the wear test as Coefficient of wear in g/N*cm are displayed in Table (4.8).

Table 4.7. Wear rate level and parameters.

Level	**Time(min)**	**Speed(m/s)**	**Load(N)**
1	5	2.827	5
2	10	2.827	10
3	15	2.827	15

Table 4.8. Values of wear coefficient.

WearCoefficient (g/N*cm)×10^{-8}		% Weight Fraction of TiO_2			
		0	0.1	0.3	0.5
% Weight Fraction of SiO_2	0	0.174	0.178	0.1987	0.117
	0.1	0.111	0.089	0.103	0.036
	0.3	0.103	0,158	0.164	0.158
	0.5	0.081	0.089	0.102	0.049

PART FIVE

RESULTS AND DISCUSSIONS

5.1. MICROSTRUCTURE FOR OPTICAL ANDMICROSCANING (SEM)

The uniform dispersion of the reinforcing particles is the most critical component for achieving a homogenous quality in discontinuous reinforced composite materials. The microstructure in the sample matrix is virtually spherical, as seen in Figures (5.1 to 5.9), and its distribution is relatively uniform. The interface layer among the matrix and the reinforcement particles should promote hydration because the Contact concerning the reinforcement particles and Al-melt. In matrix metallic compounds (MMCs), Because of the strong bonding that permits the transfer and distribution of the load from the matrix to the reinforcement, the interfacial Contact among the matrix metal and the reinforcement is important [65].

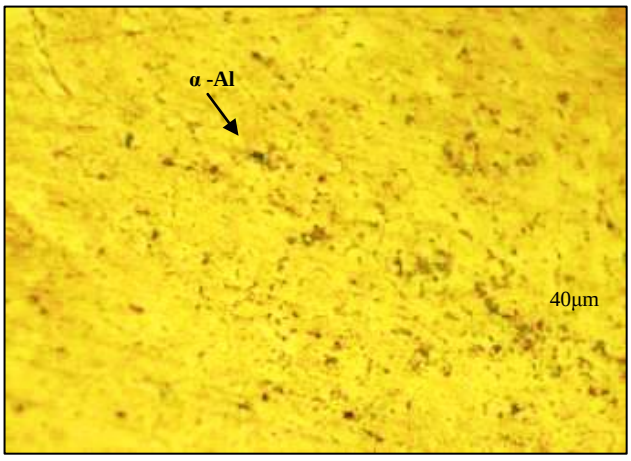

Figure 5.1. Thebase alloy microstructure.40X

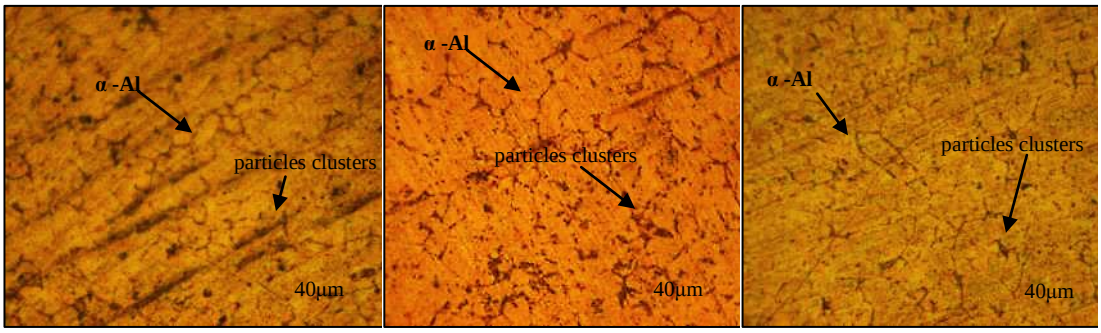

(a) (b) (c)

Figure 5.2. (A) Base Alloy+ 0.1%TiO_2, (B) Base Alloy+ 0.1%SiO_2, (C) Base Alloy+0.1% (TiO_2, SiO_2). 40X

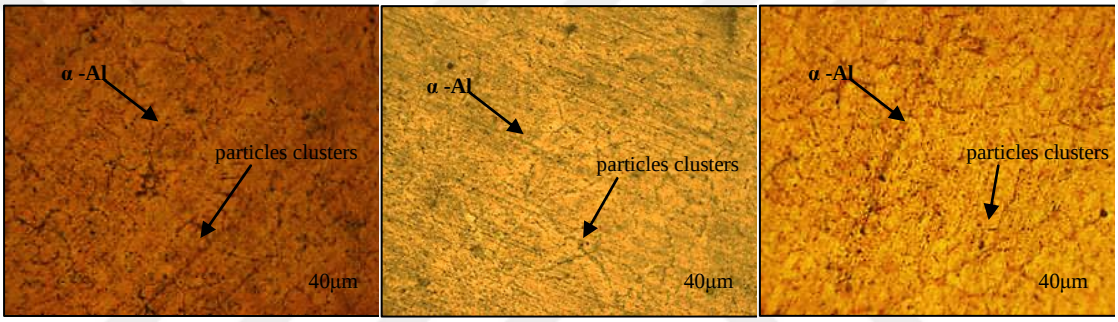

(a) (b) (c)

Figure 5.3 (A) Base Alloy+0.3%TiO_2, (B) Base Alloy+0.3%SiO2, (C) Base Alloy+0.3% (TiO_2, SiO2).40X

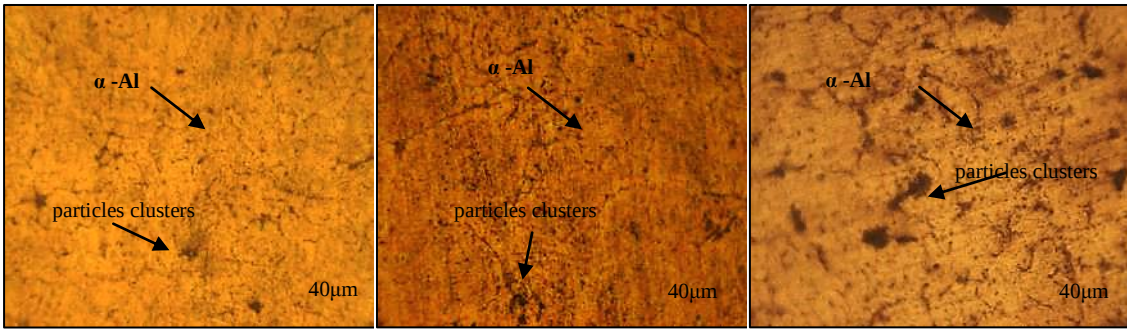

(a) (b) (c)

Figure 5.4. (A) Base Alloy+0.5%TiO_2,(B) Base Alloy+0.5%SiO_2, (C) Base Alloy+0.5% (TiO_2, SiO_2).40X

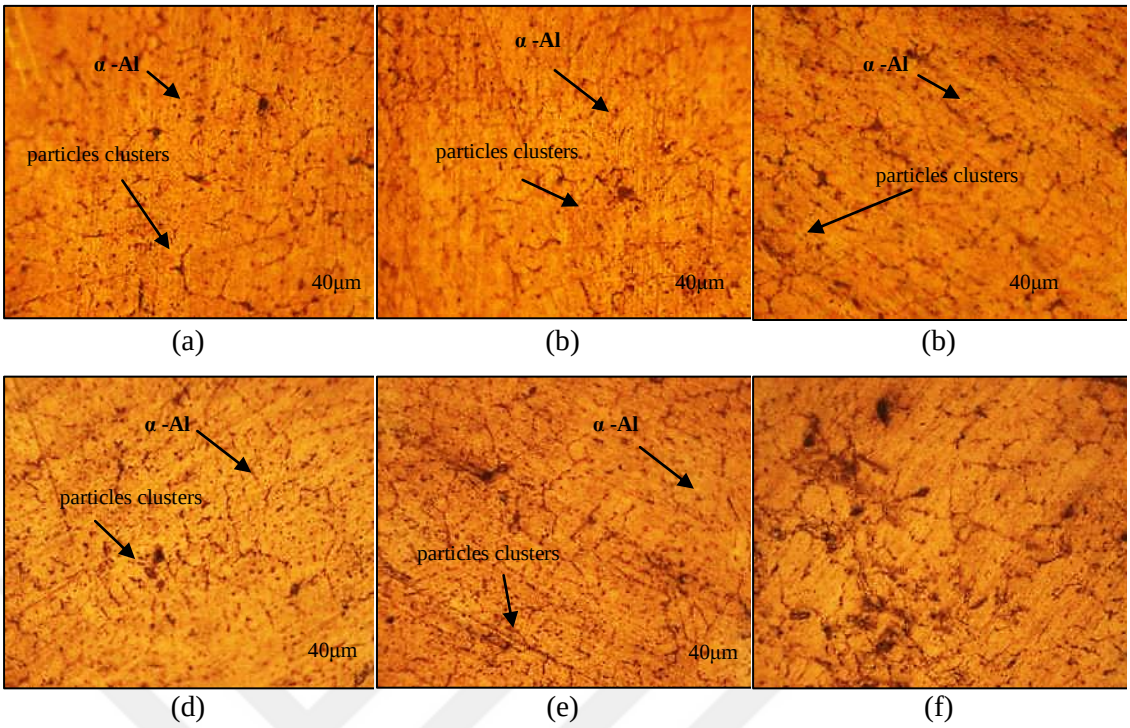

Figure 5.5 (A) Hybrid Composite 0.1%TiO_2+ 0.5%SiO_2,(B) 0.1%TiO_2+ 0.3%SiO_2, (C) 0.3%TiO_2+ 0.1%SiO_2, (D) 0.3%TiO_2+ 0.5%SiO_2, (E) 0.5%TiO_2+ 0.3%SiO_2,(F) 0.5%TiO_2+ 0.1%SiO_2.40X

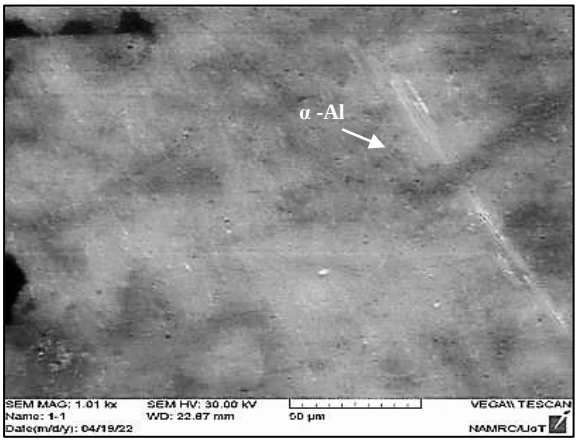

Figure 5.6. SEM for the base alloy.

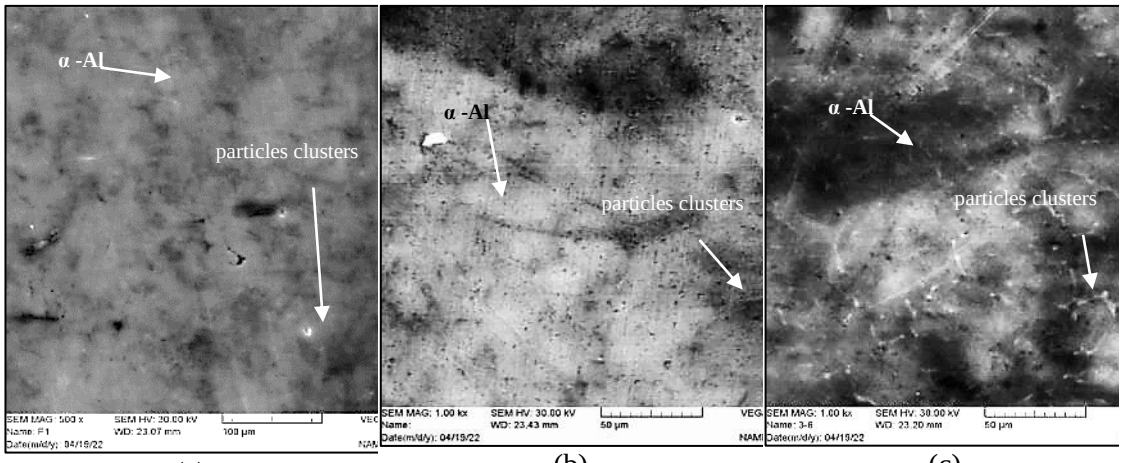

(a) (b) (c)

Figure 5.7. SEM For (A) Base Alloy+0.1%TiO_2, (B) Base Alloy+0.1%SiO_2, (C) Base Alloy+0.1% (TiO_2, SiO_2).

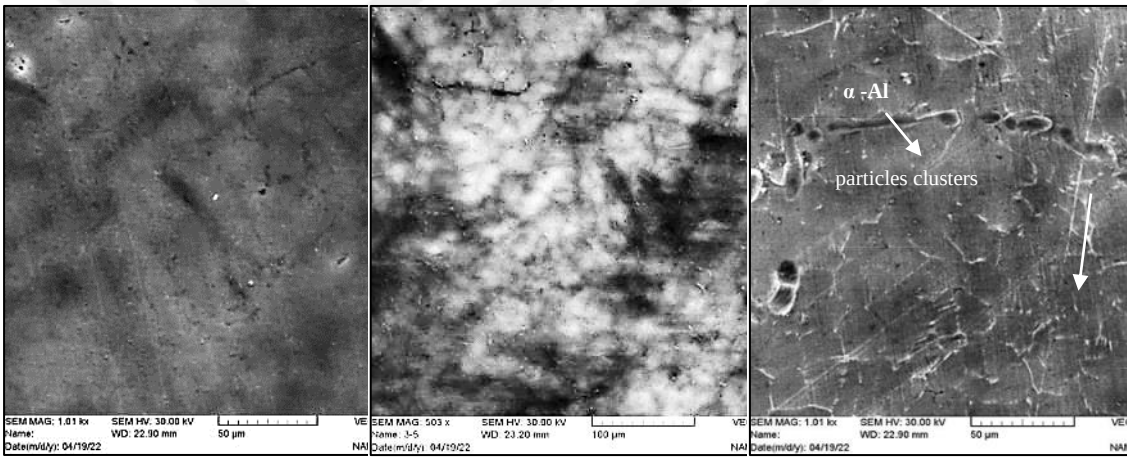

(a) (b) (c)

Figure 5.8. SEM For (A) Base Alloy+ 0.3%TiO_2, (B) Base Alloy+0.3%SiO_2, (C) Base Alloy+0.3% (TiO_2, SiO_2).

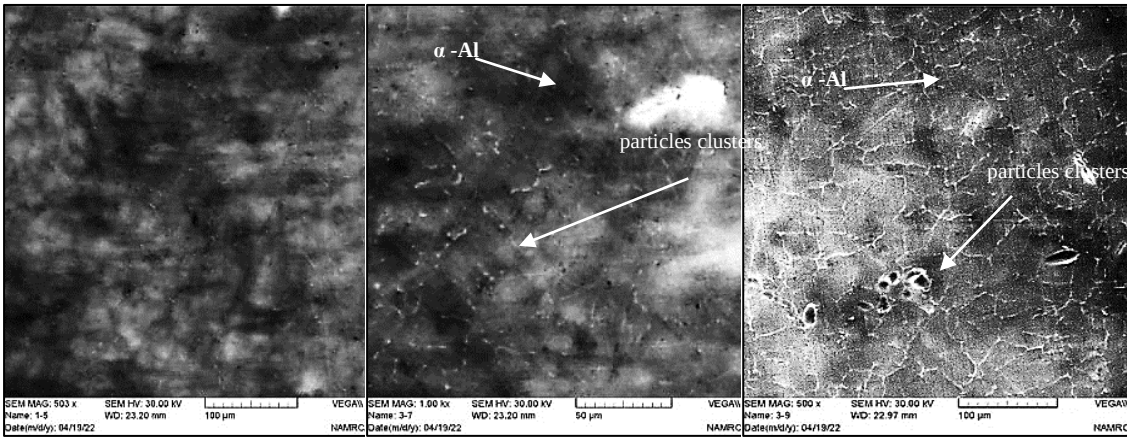

(a) (b) (c)

Figure 25.9. SEM For (A) Base Alloy+0.5%TiO_2,(B) Base Alloy+0.5%SiO_2, (C) Base Alloy+0.5% (TiO_2, SiO_2).

5.2. X-RAY DIFFRACTION INSPECTION

The graphs were created using an investigation of the base aluminum alloy reinforced with 0.5 wt% TiO_2 and SiO_2. In that order, the reinforcing materials were first added individually and then added together (hybrid). Figures (5.10 to 5.15)display the data of the phase analysis of the generated phases. The α-Al phase and compounds (TiO_2, SiO_2) were deposited, which canbeObserved in the tables attached to the drawings.This helped the composite material's yield strength and stiffness values rise.

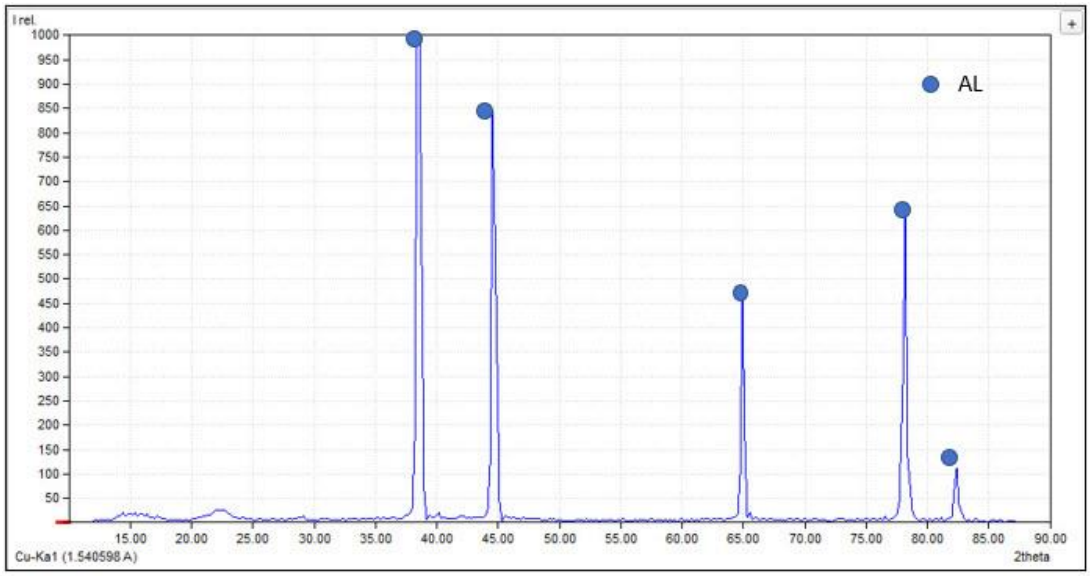

Figure 5.10.X-Ray diffraction for the al-6061 alloy.

Table 5.1. Result of XRD examination for Al-6061 alloy.

Θ standard	**Θ measured**	**(h k l)**	**Int standard**
38.472˚	38.50	(111)	100
44.738˚	44.70	(200)	47
65.133˚	65.08	(220)	22
78.227˚	78.23	(311)	24
82.435˚	82.44	(222)	17

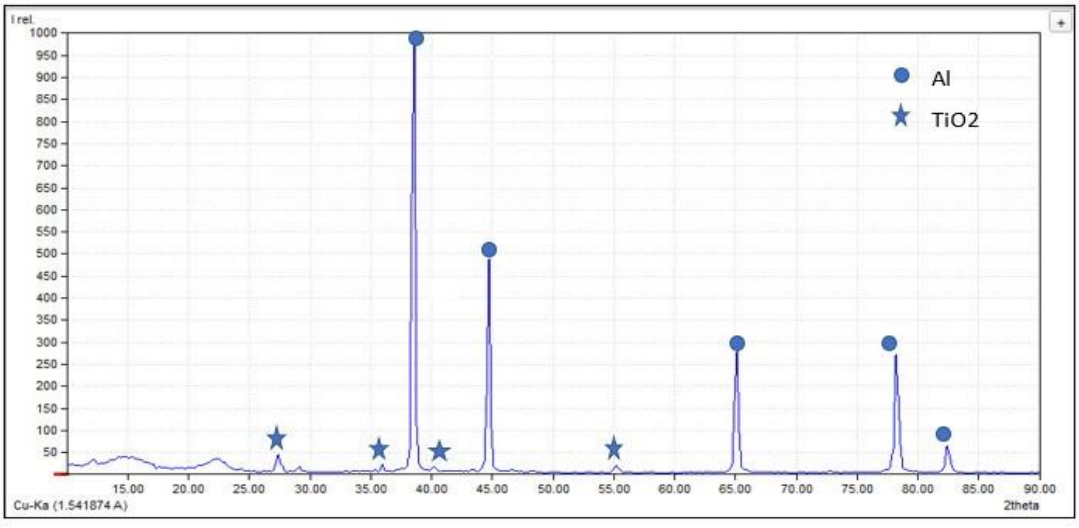

Figure 5.11. 0.5% TiO_2 compositex-ray diffraction analysis.

Table 5.2. Result of XRD examination for composite 0.5% TiO_2.

Θ standard	**Θ measured**	**(h k l)**	**Int standard**
27.446˚	27.43	(1 1 0)	100
36.085˚	36.12	(1 0 1)	50
38.472˚	38.53	(111)	100
41.225˚	40.18	(1 1 1)	25
44.738˚	44.77	(200)	47
54.322˚	54.24	(21 1)	60
56.640˚	55.26	(2 20)	20
65.133˚	65.7	(220)	22
78.227˚	78.28	(311)	24
82.435˚	82.47	(222)	17

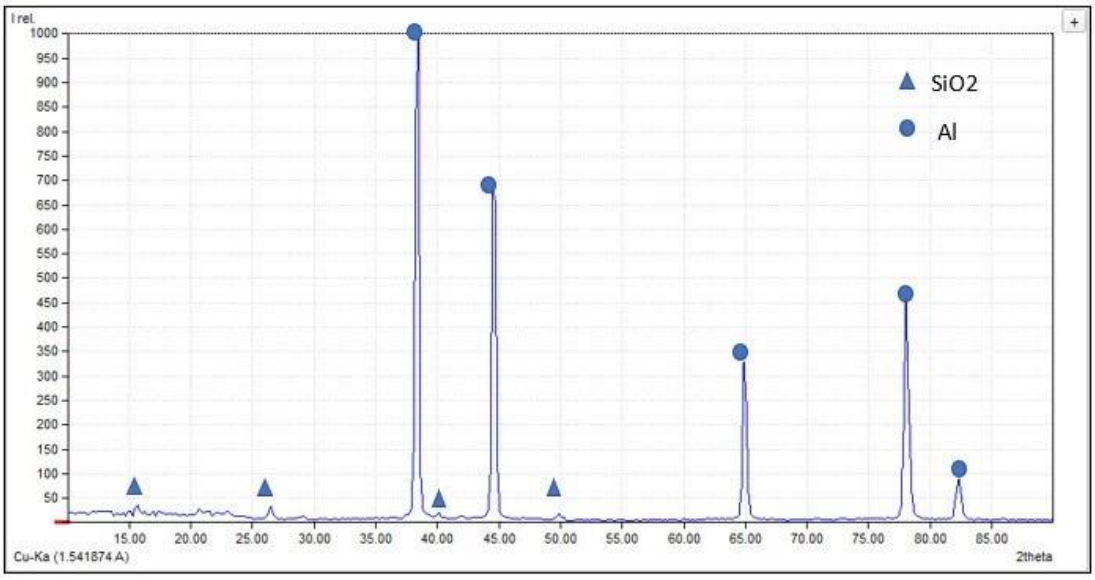

Figure 35.12. 0.5% SiO_2 compositex-ray diffraction analysis.

Table 5.3. Result of XRD examination for composite 0.5% SiO_2.

Θ standard	Θ measured	(h k l)	Int standard
20.860˚	21.13	(100)	16
26.639˚	26.51	(101)	100
38.472˚	38.42	(111)	100
44.738˚	44.62	(200)	47
50.138˚	49.86	(112)	13
65.133˚	65	(220)	22
78.227˚	78.15	(311)	24
82.435˚	82.36	(222)	17

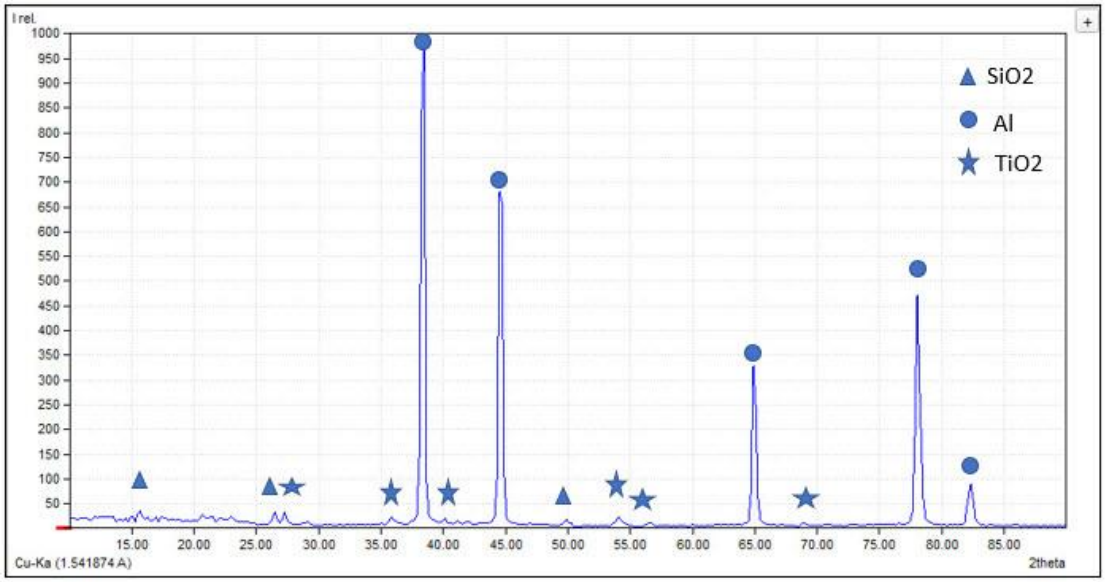

Figure 5.13. 0.5% hybrid compositex-ray diffraction analysis.

Table 5.4. The result for the XRD examination of 0.5% hybrid composite.

Θ standard	Θ measured	(h k l)	Int standard
20.860˚	20.85	(100)	16
26.639˚	26.93	(101)	100
27.446˚	27.22	(1 1 0)	100
36.085˚	35.99	(1 0 1)	50
38.472˚	38.48	(111)	100
41.225˚	40.31	(1 1 1)	25
44.738˚	44.64	(200)	47
50.138˚	49.88	(112)	13
54.322˚	54.18	(21 1)	60
56.640˚	56.67	(2 20)	20
65.133˚	65.11	(220)	22
78.227˚	78.19	(311)	24
82.435˚	82.39	(222)	17

5.3. HARDNESS TEST RESULTS

It was discovered that the hardness of composite materials increases as the weight fractions of the reinforcing particles increases.as a result of the rise in the resistance to the dislocation movement. This caused a significant impediment to the direction of the turbulence, and the result showed that the hybrid composite exhibited higher stiffness than the single composite materials [66].

As more ceramic particles are added to the composite, the compound becomes harder owing to the harder reinforcing particles, which enhance the resistance to localized plastic deformation by preventing turbulent movement. [67] [68], the reduction in the antiparticle space among the TiO_2 particle and the solid SiO_2 increases the accumulation of disturbances. One of the significant advantages of the dispersion strengthening effect is that it is maintained even at high temperatures and for long periods. The hardness of titanium dioxide composite reinforcement is higher than that of silicon dioxide composite reinforcement because TiO_2 has higher hardness when compared to SiO_2 and base alloys [69]. Figure (5.14) The relationship between stiffness and reinforcements.

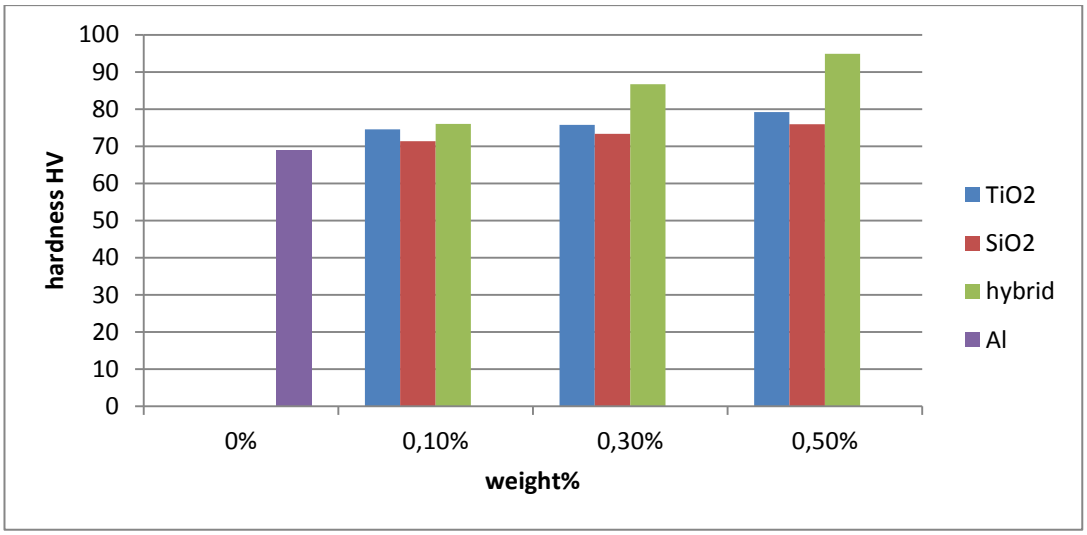

Figure 5.14. The relationship between hardness and reinforcement weight %.

5.4. TENSILE TEST RESULTS

The base alloys' tensile strength and composites have been performed at constant stress. According to the results, depending on the type of hardened filler particles applied to the composite and their perfect bonding, the tensile value and yield strength of the composite are more extensive than those of the primary alloys (non-reinforced), showing the matrix and particles, in addition to according to X-ray, the nanoparticle purification improves the strength of the composites, alien presence of the compounds TiO_2 and SiO_2. The distribution of these materials within the base alloy and the differences in the thermal expansion coefficients of the matrix and the ceramic particles increase the dislocation density in the mixture [70].in order the dislocations to pass through the matrix phase's dispersed particle population. These particles act as barriers against the deformation of the base alloy because of the effective cohesion among the filler particles and the basic alloy caused by the high resistance of the interfacial bond, enabling the load to move between the base alloy and the reinforcement particles ($SiO_2$and TiO_2).Since the ceramic particles make the material more brittle, it is clear that the elongation reduces [70]. The stress-strain curve of Al, $0.1TiO_2$, $0.1SiO_2$, and 0.1 hybrids is shown in Figure (5.15) below.

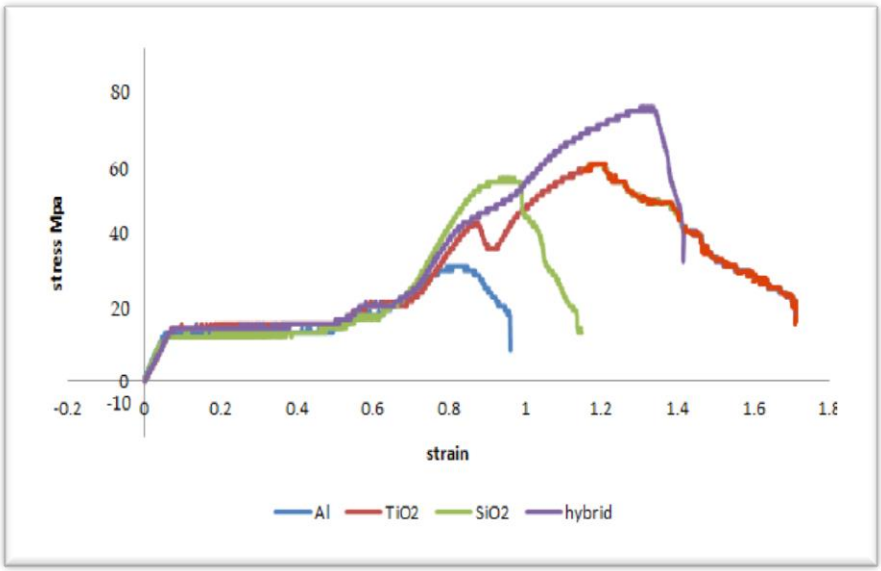

Figure 5.15. Stress-strain curve for al, $0.1TiO_2$, $0.1SiO_2$, 0.1 hybrid.

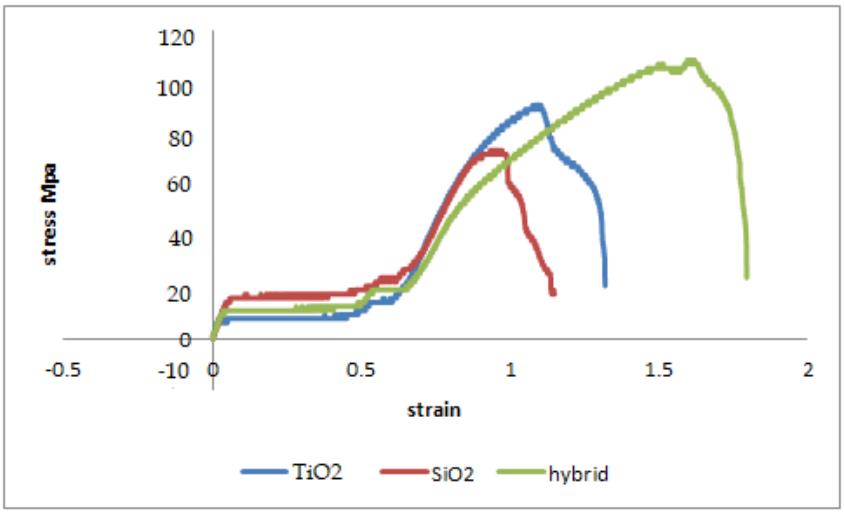

Figure 5.16. Stress-strain curve for 0.3 TiO_2, 0.3 SiO_2, 0.3 hybrid.

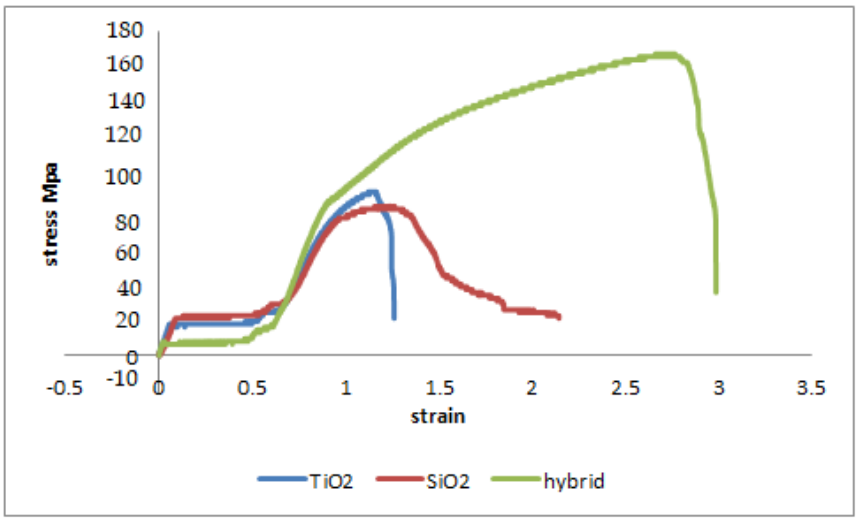

Figure 45.17. Stress-strain curve for 0.5 TiO_2, 0.5 SiO_2, 0.5 hybrid.

The effects of wt.% reinforcement on the yield strength, elongation, and ultimate tensile strength of the aluminum matrix and composites are illustrated in figures 5.18 to 5.20.

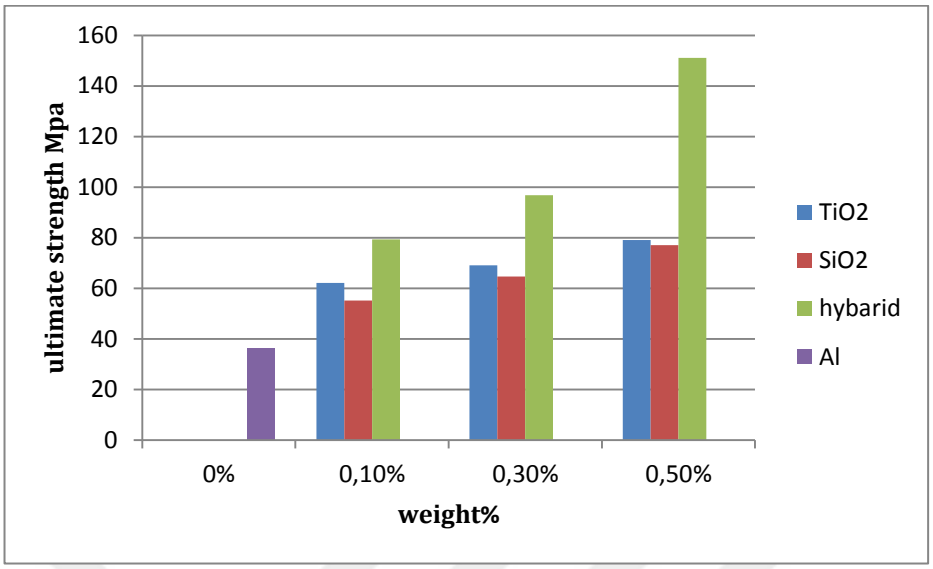

Figure 5.18.Effect of adding weight % reinforcement on ultimate strength.

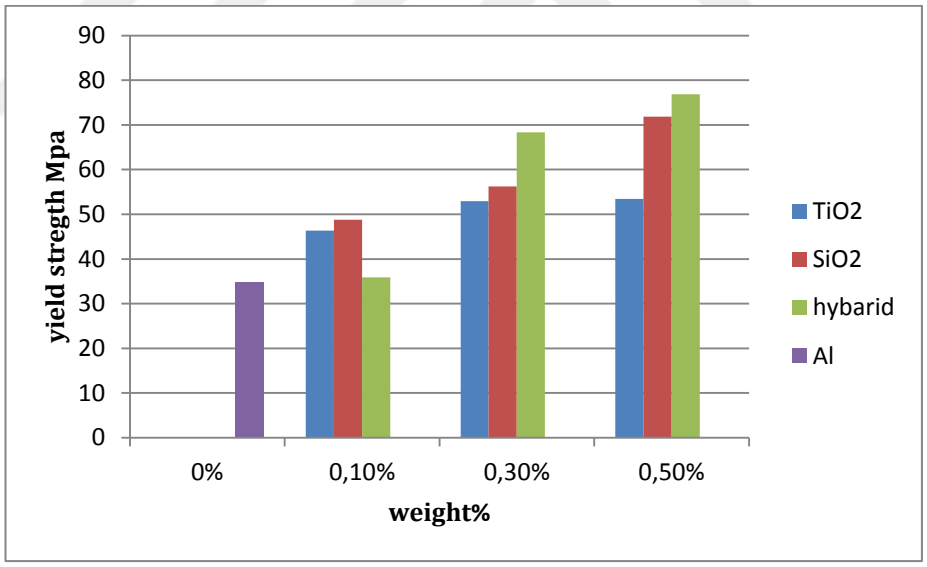

Figure 5.19. Effect of adding weight % reinforcement on yield strength.

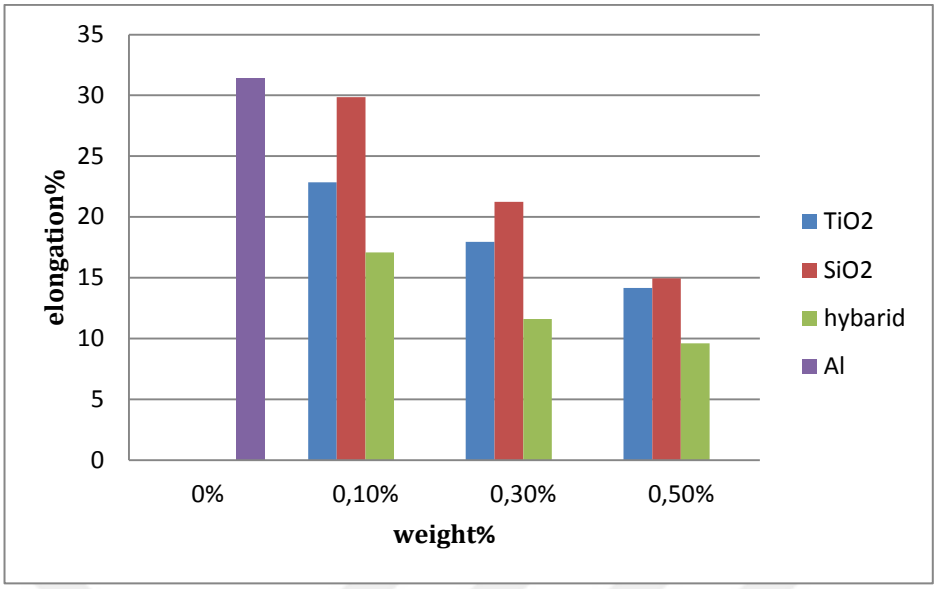

Figure 5.20. Effect of adding weight % reinforcement on elongation.

The stress localization at the acute angles of the particles was considered the dominant source of the fracture initiation method in those compounds. Thus, The matrix's ductile fracture is caused by the binding mechanism's failure, which results in the Creation of the grooves seen on the specimen surface [71]. The SiO_2 particles and the aluminum alloy matrix have a weaker connection due to particle aggregation. Compared to a matrix of elastically and plastically deformed aluminum alloy particles, larger particles transmit loads more effectively. A crack may form as a result of this. Cracking is also caused by the presence of porosity. In light of this, it is evident that MMC fracture samples have brittle fractures [72].

5.5. WEAR TEST RESULTS

Dry wear tests were performed on the base alloy, and hybrid composites. The samples' weight loss is analyzed by discovering the final and initial weight differences. All tested models' measured weight loss values were converted into wear rate.

Studying how SiO_2 and TiO_2 affect the stability of sliding velocity and changes in load and time was done using weight loss data from the alloy sample and then calculate the wear value of the base alloy, unformed reinforced composites, and hybrid composite materials.

The effect of the additional weight%going on the wear rate of the base alloys and compounds was studied at the different loads (15, 10, and 5 N) and constant sliding speeds (2.8 m/sec) with the different times (15, 10, and 5 minutes). Figures (5.21 to 5.23) show the effect of adding weight % reinforcement on wear rate. In both base alloys and composites, the rate of wear is negatively correlated with the weight % increase of the reinforcing particles.The reason is that increasing the ratio of TiO_2 and SiO_2 reduced the wear rate, because of plastic deformation, which causes the wear rate to be inversely proportionate to the hardness.

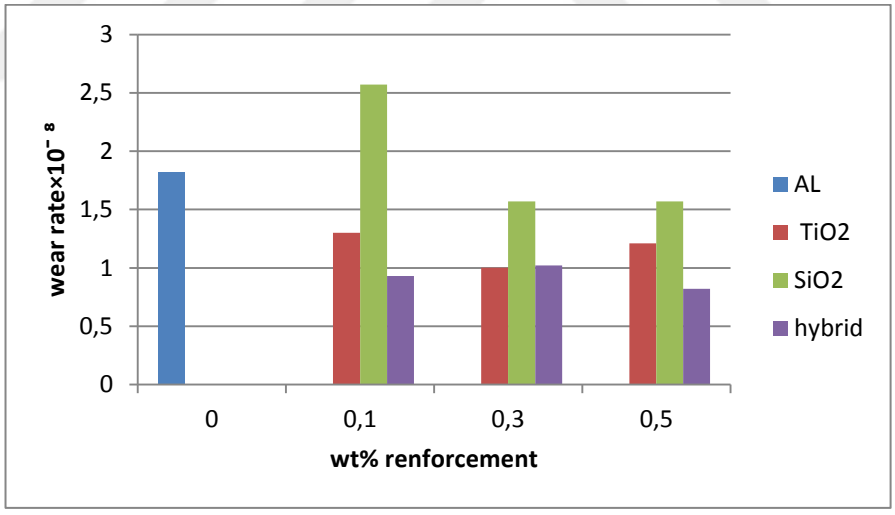

Figure 5.21. Effect of adding weight % reinforcement on wear rate at load 5N time 5min and sliding speed 2.8 m/sec.

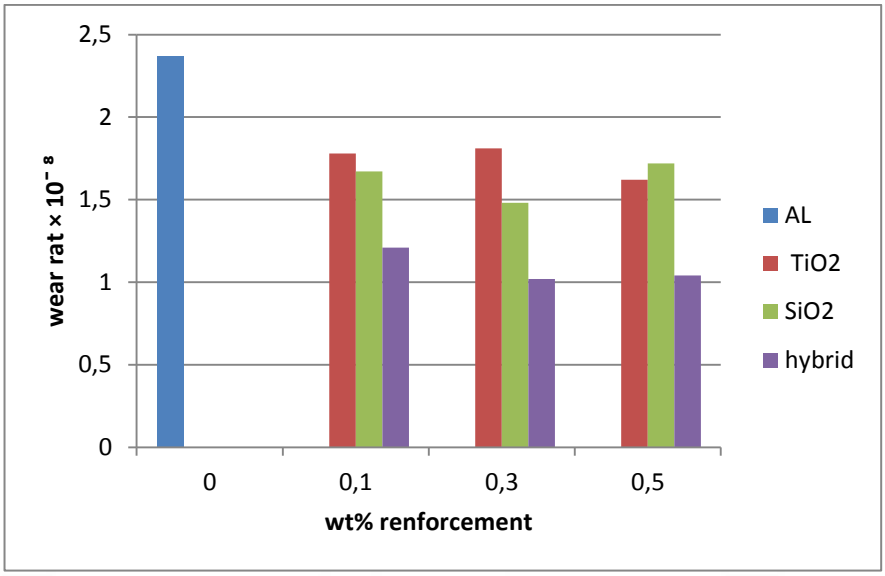

Figure 5.22 Effect of adding weight % reinforcement on wear rate at load 10N time 10min and sliding speed 2.8 m/sec.

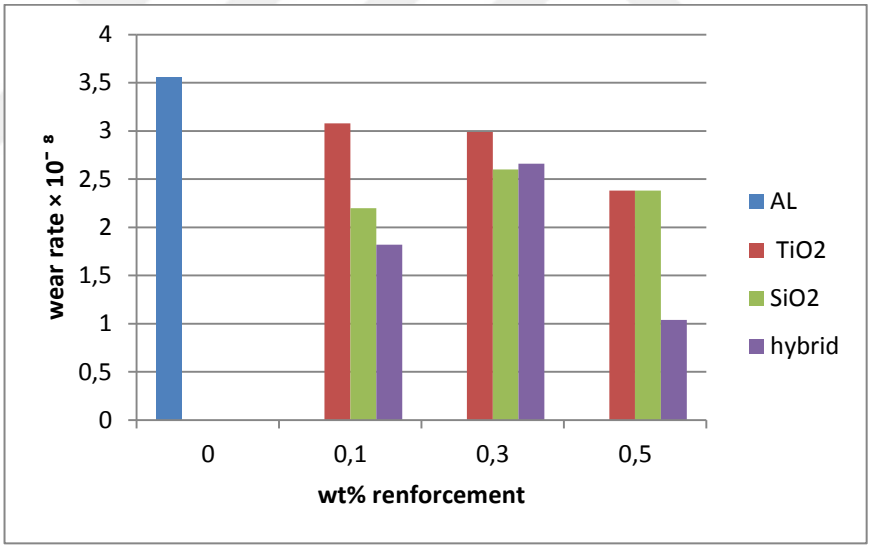

Figure 5.23. Effect of adding weight % reinforcement on wear rate at load 15N time 15min and sliding speed 2.8 m/sec.

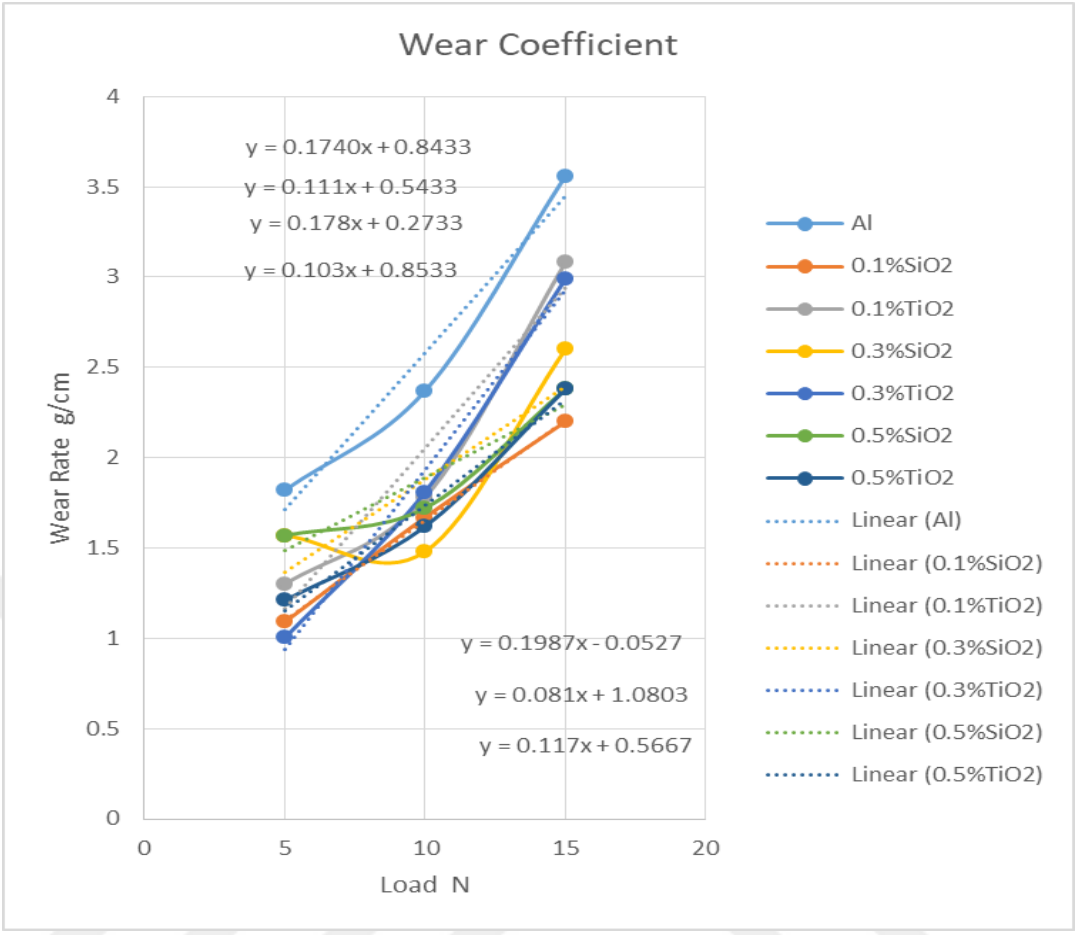

Figure 5.24. Effect of increasing the load on wear rate.

Using optical microscopy on samples of the base alloy and compounds after wear tests, Figures (5.25 -5.27) show the load's effect on these samples. The worn surfaces consist mainly of longitudinal grooves and partially irregular pits. By examining the microstructure, it can be concluded that adhesive wear may be seen on the surface of most abrasive materials. According to the figures the load has increased, The surface of the base and composite samples show an increase in wear residue. We noticed that the sloping tracks are close and not deep when the loads are low and that due to the heat generated, An oxide layer covers some places. which indicates the presence of oxidative corrosion. The width of the wear lines increases and turn out to groove with increasing loads, the surface of the models was covered with both little and huge cracks. In addition, some titanium oxide or silicon oxide particles leave the ground and move as a third form between the piece and hard disk as they continue to slide. The deformation of the sample surface increases with a higher load. Some

particles may be pushed up due to their hardness within a soft matrix, causing more significant distortion of the sample surface [73, 74, 75].

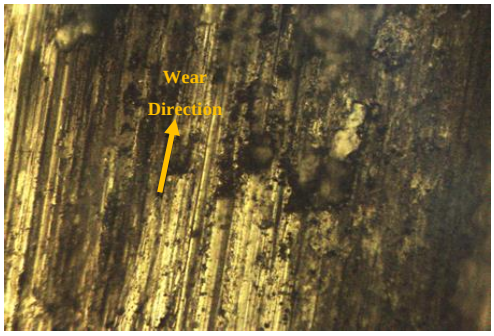

Figure 55.25. The microstructure of al-6061 after wear test. 10X

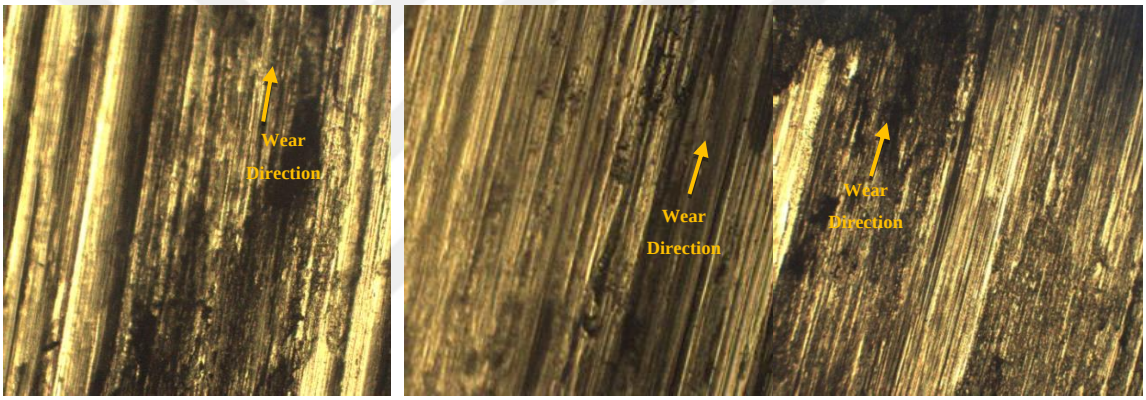

(a) (b) (c)

Figure 5.26 (A) Al-6061+0.1%TiO_2, (B) Al-6061+0.1%SiO_2, (C) Al-6061+0.1% (TiO_2,SiO_2) at load 5n time 5min and sliding speed 2.8 M/Sec.10X

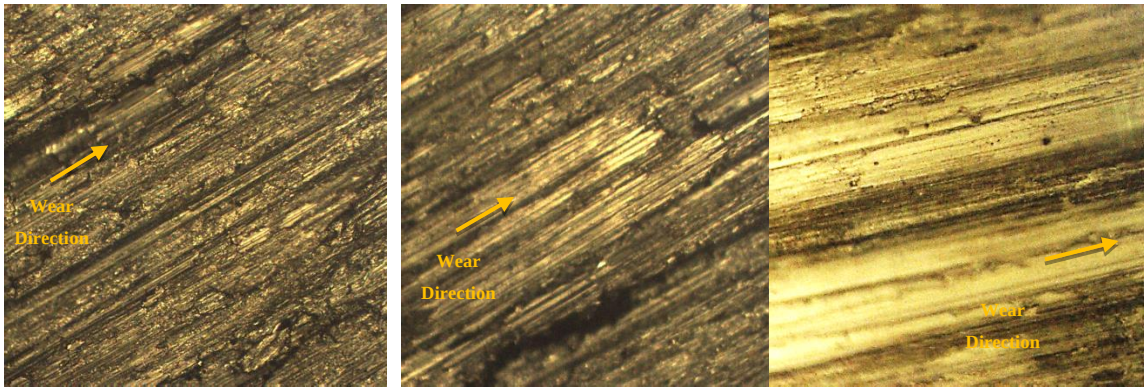

(a) (b) (c)

Figure 5.27. (A) Al-6061+0.3%TiO_2, (B) Al-6061+0.3%SiO_2, (C) Al-6061+0.3% (TiO_2,SiO_2)at load 10n time 10min and sliding speed 2.8 M/Sec.10X

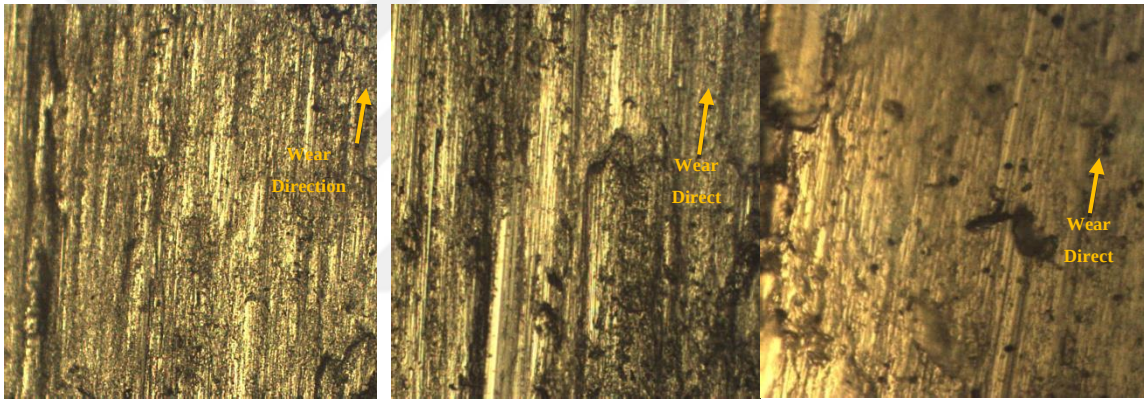

(a) (b) (c)

Figure 5.28. (A) Al-6061+0.5%TiO_2, (B) Al-6061+0.5%SiO_2, (C) Al-6061+0.5% (TiO_2,SiO_2) at load 15n time 15min and sliding speed 2.8 M/Sec.10X

PART SIX

CONCLUSIONS AND RECOMMENDATIONS

6.1. CONCLUSIONS

The researcher reached essential conclusions in this research, which are as follows:

- A homogeneous reinforced particle distribution in the Al 6061 matrix was obtained from a stir casting process.
- With an increase in the weight of titanium dioxide and silica, the hardness of the base compound alloy and the hybrid composites increases. The amount of hardness when 0.5wt% of the hybrid composite was added became 77.35HV compared to 68.88HV in the base alloy.
- With the increase of the additions of TiO_2 and SiO_2, the yield strength and ultimate tensile strength of the single and hybrid composites increased. When 0.5 hybrid compound was added, the tensile strength became 151.12 MPa,as 317% and the yield strength became 76.87 MPa as 120% with respect that with the base alloy.
- elongation decreasedwith the increase of TiO_2 and SiO_2 additions. When adding 0.5wt% hybrid composite, the amount of elongation became 9.61% compared to 31.39% in the base alloy.
- The wear rate of the hybrid composite with 0.5% TiO_2 and 0.5% SiO_2 shows a lower wear rate. And it was worth0.82×10^{-8}gm/cm compared to 1.82×10^{-8} gm/cm in the base alloy.
- 6- Compared to the sliding time and speed, the applied load is the most significant factor affecting the wear rate, as studies have shown.

6.2. RECOMMENDATIONS

After conducting all theoretical and practical experiments on alloys (Al 6061) and composite materials, the researcher suggests the following recommendations:

- Studying effect of adding ZrO_2 + graphite on the properties of the hybrid nanocomposite.
- Optimize the load, slip speed and distance effect on Hybrid nanocomposite.
- Study the development of various$SiO_2$and TiO_2 nanoparticles on impact and corrosion resistance.
- Studying the effect of adding (SiO_2andTiO_2) nanoparticles to aluminum alloys produced by recasting on microstructure and properties.

REFERENCES

1. Aluminum and aluminum alloys /edited by J.R. Davis; prepared under the direction of the ASM International Handbook Committee. p. cm. **ASM speciality handbook** Includes bibliographical references and index.

2. Corrosion of Aluminum and Aluminum Alloys Copyright **1999 ASM International** J.R. Davis, editor, p 1-24. All rights reserved. DOI: 10.1361/caaa1999p001.

3. **Alloying: Understanding the Basics** J.R. Davis, p351-416 DOI:10.1361/autb2001p351.

4. Corrosion Tests and Standards: **Application and Interpretation**, R.Baboian, Ed., ASTM,1995.

5. D.G. Altenpohl, Aluminum: Technology, Applications, and Environment, 6th ed., **The Aluminum Association Inc.** and TMS, 1998.

6. Kearney, A.L.: Properties of cast aluminum alloys. In: ASM Handbook, Properties and Selection: **Nonferrous Alloys and Special-purpose Materials**, vol. 2, pp. 152–177. ASM International (1990).

7. Baradarani, B., Raiszadeh, R.: **Precipitation hardening of cast Zr-containing A356 aluminiumalloy**. Mater. Des. 32, 935–940 (2011).

8. Clyne, T.W., Withers, P.J. **An Introduction to Metal Matrix Composites**. Cambridge University Press, Cambridge (1995).

9. Friedlander, J.N.: **Metal Matrix Composites**. Springer, Netherlands (1994).

10. Manna, A., Bhattacharyya, B**.: A study on machinability of Al/SiC-MMC. J. Mater. Process.Technol.** 140, 711–716 (2003). doi:10.1016/S0924-0136(03)00905-1

11. Ellis, M.B.D.: **Joining of aluminium based metal matrix composites**. Int. Mater. Rev. 41,41–58 (1996). doi:10.1179/095066096790326066.

12. Rotundo, F., Ceschini, L., Morris, A., et al.: **Mechanical and microstructural characterization of2124Al/25 vol.%SiCp joints obtained by linear friction welding(LFW)**. Compos. Part A 41,1028–1037 (2010). doi:10.1016/j.compositesa.2010.03.009.

13. Ceschini, L., Morri, A., Rotundo, F.: **Forming of metal matrix composites**. Comp. mater. Process. Adv. Form. Technol. 3 (2014).

14. D. D. Chung, Composite Materials**, Science and Applications**, Second Edition, London, 2010.

15. Alwan, otbah H., **A study on the reciprocating wear behavior of aluminum alloy / SiC composite under dry and wet conditions**, Baghdad, Iraq, M.Sc. thesis, 2014.

16. Singh, Anurag, processing, characterization and sliding wear behavior of functionalized carbon nanotube reinforced epoxy matrix composite**, National Institute of Technology**, Rourkela, Odisha, India, 2014.

17. Nikhilesh Chawla, Krishan K. Chawla **METAL MATRIX COMPOSITES Arizona State University**, Tempe, AZ, University of Alabama at Birmingham, AL, 2006.

18. Uju, Williams Alozie, **Synchrotron X-Ray Absorption Spectroscopy And Thermal Analysis Study Of Particle-Reinforced Aluminium Alloy Composites**, University of Saskatchewan, Canada, 2009.

19. Krishan K. Chawla, Composite Materials Science and Engineering Third Edition University of Alabama at Birmingham, AL 35294, USA **kchawla@uab.edu,** 1998.

20. Hamedan, A.D., Shahmiri, M.: **Production of A356–1wt% SiC nanocomposite by the modified stir casting method. Mater Sci Eng** A 556, 921–926 (2012). doi:10.1016/j.msea. 2012.07.09.

21. Surappa, M.K.: **Aluminum matrix composites**: challenges and opportunities. Sadhana 28,319–334 (2003).

22. Suresh, S.M., Mishra, D., Srinivasan, A. et al.: **Production and characterization of micro and nano Al2O3 particle-reinforced LM25 aluminum alloy composites**. 6, 94–98 (2011).

23. Prasad, Naresh, **development and characterization of metal matrix composite using red mud an industrial waste for wear resistant applications**, National Institute of Technology, India, 2006.

24. Donthamsetty, S., Damera, N.R., Jain, P.K.: **Ultrasonic cavitation assisted fabrication and characterization of A356 metal matrix nanocomposite reinforced with Sic**, B4C, CNTs. AIJSTPME 2, 27–34 (2009).

25. Cao, G., Konishi, H., Li, X.: **Mechanical properties and microstructure of SiC-reinforced Mg-(2,4)Al-1Si nanocomposites fabricated by ultrasonic cavitation-based solidification processing. Mater Sci Eng** A 486, 357–362 (2008). doi:10.1016/j.msea. 2007.09.054.

26. Rohatgi, P., Guo, R., Iksan, H., et al.: **Pressure infiltration technique for synthesis of aluminum–fly ash particulate composite. Mater Sci Eng** A 244, 22–30 (1998). doi:10.1016/ S0921-5093(97)00822-8.

27. Suryanarayana, C., Al-Aqeeli, N**.: Mechanically alloyed nanocomposites. Prog Mater Sci** 58,383–502 (2013). doi:10.1016/j.pmatsci.2012.10.01.

28. Cintas, J., Cuevas, F.G., Montes, J.M., Herrera, E.J.: **High-strength PM aluminium by milling in ammonia gas and sintering. Scr Mater** 53, 1165–1170 (2005). doi:10.1016/j.scriptamat.2005.07.019.

29. Fan, Z.: **Semisolid metal processing. Int Mater Rev** 47, 49–86 (2002). doi:10.1179/095066001225001076.

30. Sankaranarayanan, S., Sabat, R.K., Jayalakshmi, S., et al.: **Effect of hybridizing micron-sized Ti with nano-sized SiC on the microstructural evolution and mechanical response of Mg–5.6 Ti composite.** J Alloys Compd 575, 207–217 (2013). doi:10.1016/j.jallcom.2013.04.095.

31. Sajjadi, S.A., Ezatpour HR, H.R., Torabi Parizi, M.: **Comparison of microstructure and mechanical properties of A356 aluminum alloy/Al2O3 composites fabricated by stir and compo-casting processes.** Mater Des 34, 106–111 (2012). doi:10.1016/j.matdes.2011.07.037.

32. Sajjadi, S.A., Ezatpour, H.R., Beygi, H**.: Microstructure and mechanical properties of Al–Al2O3 micro and nanocomposites fabricated by stir casting**. Mater Sci Eng A 528, 8765–8771 (2011). doi:10.1016/j.msea.2011.08.052.

33. Ezatpour, H.R., Sajjadi, S.A., Sabzevar, M.H., Huang, Y.: **Investigation of microstructure and mechanical properties of Al6061-nanocomposite fabricated by stir casting**. Mater Des 55, 921–928 (2014). doi:10.1016/j.matdes.2013.10.060.

34. Karbalaei Akbari, M., Mirzaee, O., Baharvandi, H.R.: **Fabrication and study on mechanical properties and fracture behavior of nanometric Al2O3 particle-reinforced A356 composites focusing on the parameters of vortex method**. Mater Des 46, 199–205 (2013). doi:10.1016/ j.matdes.2012.10.008.

35. So, K.P., Jeong, J.C., Park, J.G., et al.: **SiC formation on carbon nanotube surface for improving wettability with aluminum. Compos Sci Techno**l 74, 6–13 (2013). doi:10.1016/ j.compscitech.2012.09.014.

36. Sanaty-Zadeh, A.: **Comparison between current models for the strength of particulate-reinforced metal matrix nanocomposites with emphasis on consideration of Hall-Petch effect.** Mater Sci Eng A 531, 112–118 (2012). doi:10.1016/j.msea.2011.10.043.

37. Mazahery, A., Abdizadeh, H., Baharvandi, H.R.: **Development of high-performance A356/nano-Al2O3 composites**. Mater Sci Eng A 518, 61–64 (2009). doi:10.1016/j.msea.2009.04.14.

38. Yar, A., Montazerian, M., Abdizadeh, H., Baharvandi, H.R.: **Microstructure and mechanical properties of aluminum alloy matrix composite reinforced with nanoparticle** MgO. J Alloys Compd 484, 400–404 (2009). doi:10.1016/j.jallcom.2009.04.117.

39. Alizadeh, A., Hajizamani, M.: **Hot extrusion process effect on mechanical behavior of stir cast al based composites reinforced with mechanically milled B 4 C nanoparticles**. J Mater Sci Technol 27, 1113–1119 (2011). doi:10.1016/S1005-0302(12)60005-X.

40. Wang, D., De Cicco, M.P., Li, X.: **Using diluted master nanocomposites to achieve grain refinement and mechanical property enhancement in as-cast Al–9Mg**. Mater Sci Eng A 532, 396–400 (2012). doi:10.1016/j.msea.2011.11.002.

41. Abbasipour, B., Niroumand, B., Monirvaghefi, S.: **Mechanical properties of A356-CNT cast nanocomposite**. Suppl Proc Mater Process Interfaces 1, 733–740 (2012).

42. Purushothaman, S., Tien, J.K.: **Role of back stress in the creep behavior of particle strengthened alloys**. Acta Metall. 26, 519 (1978).

43. Fernández, R., González-Doncel, G.: **Threshold stress and load partitioning during creep of metal matrix composites**. Acta Mater 56, 2549–2562 (2008). doi:10.1016/j.actamat.2008.01.037.

44. Li, Y., Mohamed, F.A.: **An investigation of creep behavior in a SiC-2124 Al composite**. Acta Mater. 45, 4775–4785 (1997).

45. Choi, H.J., Bae, D.H. **Creep properties of aluminum-based composite containing multi-walled carbon nanotubes**. Scr Mater 65, 194–197 (2011). doi:10.1016/j.scriptamat. 2011.03.038.

46. Cadek, J., Kucharova, K., Sustek, V.: A PM 2124Al-20SiC p composite: **disappearance of true threshold creep behaviour at high testing temperatures**. Scr Mater 40, 1269–1275 (1999).

47. Lin, Z., Li, Y., Mohamed, F.A.: **Creep and substructure in 5 vol.% SiC–2124 Al composite**. Mater Sci Eng A 332, 330–342 (2002). doi:10.1016/S0921-5093(01)01760-9.

48. Nikhilesh Chawla., Krishan K. Chawla .: **metal matrix composites**. ISBN 10 0-387-23306-7 (2006).

49. Chawla, K.K., (1998) Composite Materials**: Science and Engineering**, Springer-Verlag, p. 276.

50. Zhang, Z.F., L.C. Zhang, and Y.W. Mai, (1995) **J. Mater. Sci**., 30, 1961-1966.

51. Garcia-Cordovilla, C., J. Narciso, and E. Louis, (1996) **Wear,** 192, 170.

52. Hosking, F. M., F. Folgar-Portillo, R. Wundnerlin, and R. Mehrabian,

(1982) J. **Mater. Sci**., 17,477.

53. Venkataraman, B., and G. Sundarajan, (1996b) **Acta Mater**., 44 461-473.

54. Venkataraman, B., and G. Sundarajan, (1996a) **Acta Mater**., 44 451-460.

55. Rohatgi, P.K., S. Ray, Y. Liu, (1992) **Inter. Mater**. Rev., 37, 192.

56. Jayashree P . K, G.Shankar M.C, A.Kini, Sharma S.S and R. Shetty, "Review on Effect of Silicon Carbide (SiC) on Stir Cast Aluminium Metal Matrix Composites,"**International Journal of Current Engineering and Technology**, vol. 3, no. 3, pp. 1061-1071, 2013.

57. Gibbs JW (1878) On the **equilibrium of heterogeneous substances**. Trans Conn Acad 3:343–524.

58. Starov VM, Velarde MG, Radke CJ (2007) **Wetting and spreading dynamics**, vol 138. CRC Press, Boca Raton.

59. Naidich JV (1981) In: **Cadenhead DA, Danielli JF (eds) Progress in surface and membrane science**, vol 14. Academic Press, Cambridge, pp 353–484

60. Li JG (1994) **Wetting of ceramic materials by liquid Si, Al and other metallic melts containing Ti and other reactive elements**. Rev Ceram Int 20(6):391–412.

61. Contreras Cuevas, Antonio; Bedolla Becerril, Egberto; Martínez, Melchor Salazar; Lemus Ruiz, José, Metal Matrix Composites Wetting and Infiltration, **Springer International Publishing**, ISBN 978-3-319-91853-2 , 2018.

62. Banerji A, Rohatgi PK, Reif W (1984) **Role of the wettability in the preparation of metalmatrix composites** (a review). Metall 38:656–661.

63. S. Kumar, "Wear Behavior Of Dual Particle Size (Dps) Reinforced Aluminum Alloy", **Material Science and Metallurgical Engineering**, India, M.Sc. thesis, July 2011.

64. D. S. a. S. Mediratta, "Effect of Load and Speed on Wear Properties of Al 88-7075-Fly Ash Composite Material," **International Journal of Innovative Research in Science, Engineering and Technology**, vol. 2, no. 5, pp. 1-9,2013.

65. B.K.Raghunath, G. Elango, "Tribological Behavior of Hybrid (LM25Al + SiC+ TiO2) Metal Matrix Composites," **international conference on design and manufacturing**, no. 64, p. 671 – 680, 2013.

66. G. B. Veeresh Kumar, C. S. P. Rao and N. Selvaraj, "Mechanical and Tribological Behavior of Particulate Reinforced Aluminum Metal Matrix Composites – a review," **Journal of Minerals & Materials Characterization & Engineering**, vol. 10, no. 1, pp. pp.59-91, 2011.

67. H. Zhang, Y. Wang, S.L. Shang, C. Ravi, C. Wolverton, L.Q. Chen and Z.K. Liu, "Solvus boundaries of (meta)stable phases in the Al-Mg-Si system: First-principles phonon calculations and thermodynamic modelling," **Computer Coupling of Phase Diagrams and Thermochemistry**, no. 34, pp. 20-25, 2010.

68. Ghazi, Jameel Habeeb, "Influence of Ceramic Particles Reinforcement on some Mechanical Properties of AA 6061 Aluminium Alloy," **Eng. &Tech. Journal**, vol. 31, no. 14, pp. 2611-2618, 2013.

69. J, Madhusudhan, "CHARACTERIZATION OF HYBRID COMPOSITE AL 7075 WITH TIO + SIC," **Indian Streams Research Journal**, vol. 5, no. 5, pp. 1-10, 2015.

70. G. B. Veeresh Kumar, C.S.P.Rao, N.Selvaraj and M.S.Bhagyashekar, "Studies on Al6061-SiC and Al7075-Al2O3 Metal Matrix Composites," **Journal of Minerals & Materials Characterization & Engineering**, Vol. 9, no. No.1, pp. 43-55, 2010.

71. Reihani, R. Ehsan and S.M. Seyed, "Aging Behavior and Tensile Properties of Squeeze Cast AL 6061/SIC Metal Matrix Composites," **Scientia Iranica**, vol. Vol. 11, no. 4, pp. pp 392-397, 2014.

72. K. F. P. Rong, **Study and Development of Novel Composite Materials for the Application of Car Brake Rotor, Department of Mechanical Engineering**, Curtin University, 2014.

73. Jithin. J. and Muthu P, "Studies on Mechanical and Wear Properties of Al7075/Zircon/Fly Ash Hybrid Metal Matrix Composites", **International Conference on Current Research in Engineering Science and Technology**, pp. 15-23, 2016.

74. Hanan Karam Azeez, Effect Of TiO_2 /SiC Addition On Mechanical Properties And Wear Resistance Of Al-Mg-Si Alloy, Master Thesis, **University of Technology Department of Production Engineering and Metallurgy**, Baghdad 2017.

75. Lina S. Salim, Effect of B4C / Fly Ash Additions on Wear and Mechanical Properties of Al -Cu -Mg Alloy, Master Thesis, **University of Technology Department of Production Engineering and Metallurgy**, Baghdad 2016.

RESUME

Mustafa Khudair Mohsen AL-GBURI completed primary and secondary education in Baghdad. He completed his secondary education at Al-Kindi High School, after which he proceeded to study at the University of Technology - Department of Production and Metallurgy Engineering from 2005-2006. Then in 2008 - 2009, I finished college and started working as an Assistant Engineer at the IGO Ministry of Agriculture.